JJEE Volume X | Number X | Month 20XX | Pages XXX-XXX

Jordan Journal of Electrical Engineering

ISSN (print): 2409-9600, ISSN (online): 2409-9619

Homepage: jjee.ttu.edu.jo

Cheetah Optimization for Optimal Sizing and Placement of Distributed Generation and Capacitors

Khaled Guerraiche[1*], Abdelatif Belballi[2], Aykut Fatih Güven[3], Latifa Dekhici[4,5], Amine Abbou[6]

[1, 2, 4, 6] LDREI Laboratory, Higher School of Electrical and Energy Engineering, Oran, Algeria
E-mail: guerraiche_khaled@esgee-oran.dz
[3] Department of Energy Systems Engineering, Yalova University, Yalova, Turkey
[5] Faculty of Computer Sciences, University of Sciences and Technology of Oran, Oran, Algeria

Received: Dec 02, 2024 *Revised: Mar 10, 2025* *Accepted: Mar 23, 2025* *Available online: Apr 6, 2025*

Abstract— Renewable energy sources and energy efficiency has emerged as the backbone of sustainable energy solutions in response to the rising tide of concern over energy security and climate change. Efforts to decrease power losses are part of this. This paper investigates the application of the Cheetah optimizer, a modern metaheuristic optimization algorithm, for the optimal sizing and placement of decentralized generation units such as shunt capacitors in radial distribution networks. The primary objectives are to minimize power losses and enhance voltage profiles under varying load conditions. Unlike conventional methods, Cheetah Optimizer employs three innovative strategies with different randomization techniques to achieve a superior balance between exploration and exploitation. The algorithm's performance is validated on the IEEE 33-bus and IEEE 69-bus distribution test systems. This investigation primarily adds value by applying the methodology to the Adrar electricity distribution network in southern Algeria, demonstrating the effectiveness of these methodologies in real-world systems. Comparative analysis demonstrates that the proposed approach achieves significant improvements in loss reduction and voltage stability compared to state-of-the-art algorithms. Key findings indicate that the Cheetah optimizer delivers robust performance across different network scenarios, with a reduction in power losses by up to 37.34 % and 66.11 % on test systems and enhanced voltage stability by increasing the minimum voltage to permissible levels. Sensitivity analysis further confirms the algorithm's reliability under varying parameter settings. These results underscore the potential of the proposed approach for real-world implementation in optimizing distribution networks.

Keywords— Distribution network; Renewable energy; Cheetah optimizer; Losses optimization.

1. INTRODUCTION

In recent years, the electric power business has undergone numerous modifications. The emergence of smart grids is advantageous not only to society as a whole, including customers and various stakeholders, but also to all participants in the electric power sector [1]. Shunt capacitors (SCs) and distributed generators (DGs) are crucial components in implementing smart distribution systems. To enhance system efficiency and provide high-quality power to customers, the smart grid necessitates the use of integrated solutions for all its components [2].

Active power loss and line loading reduction; reactive power need mitigation and voltage profile improvement are just a few of the potential benefits to the power system that could result from appropriately sized and optimally placed distributed generators. Numerous researchers have suggested various optimization methods, including traditional, AI, and hybrid intelligent system approaches, as potential solutions to this issue [3]. Installing an

* Corresponding author
DOI: https://doi.org/10.5455/jjee.204-1733161680

inductor and a capacitor in radial distribution networks can reduce power loss and improve the voltage profile. Consequently, this will result in a decrease in the amount of electrical power from the feeder. Unsuitable allocation for the capacitor or inductor will lead to a decrease in the benefits of the system and affect the system's operation control. However, the optimal number, size, and locations of distributed generators and shunt capacitors have been the subject of much research in the last two decades.

Recent studies have proposed additional goals to optimize the problem of sizing and placement of distributed generators, including enhancing voltage stability, reducing operational expenses, and minimizing greenhouse gas emissions. The optimization problem is typically approached as a single-objective using analytical approaches [4] or heuristic and meta-heuristic methods, such as the equilibrium optimization algorithm [5, 6], the coyote algorithm [7], and the particle swarm optimization (PSO) [8].

In a recent paper [9], the authors used Mixed Integer Linear Programming (MILP). This method determines the stability of the voltage in radial distribution networks. In Ref [10], the authors solved the problem using a multi-objective method based on the Strong Pareto evolutionary algorithm (SPEA2). The authors determined the optimal network reconfiguration and integration of renewable distributed generator, taking into account the time sequence variation in load. The authors have proposed an improved sine-cosine algorithm [11] to address simultaneous network reconfiguration and distributed generator allocation in radial distribution networks. Afterwards, researchers developed MPSO algorithms for network reconfiguration and distributed generator integration [12]. However, the Improved Cat Swarm Optimization for Simultaneous Allocation of DSTATCOM and distributed generators in Distribution Systems has shown promising results [13]. The Rider Optimization Algorithm for Optimal distributed generator is suggested by [14]. The authors of [15] used an improved MOPSO algorithm for the optimal sizing and placement of distributed generation. In [16], the authors used the Slime Mould Algorithm. This method determines the impact of electric vehicle charging stations on radial distribution systems. Authors in [17] solved the optimal reconfiguration and renewable distributed generation using the Salp Swarm Algorithm (SSA).

Over the past two decades, researchers have extensively studied the ideal quantity, dimensions, and placements of shunt capacitors. The authors of the study by [18] used a combined optimization approach to determine the optimal capacitor allocation in radial distribution networks. The study by [19] employed the particle swarm optimization and real-Coded Genetic Algorithm (RCGA) techniques for capacitor placement and selection. By minimizing the equation for loss savings, we can identify the ideal solution. The study by [20] employed the constraint-factor particle swarm optimization to determine the ideal placement of shunt capacitors in radial distribution networks. The work by [21] introduced bio-inspired optimization algorithms for the optimal allocation of capacitor banks in radial distribution systems, aiming to minimize real power loss and maximize network savings. The multi-objective water cycle algorithm for solving the capacitor placement problem in radial distribution networks has been demonstrated by [22]. The referenced paper [23] presents the mixed-integer conic optimization technique, which determines the optimal loss reduction and capacitor placement in radial distribution networks. Ref [24] presents the optimal capacitor placement in distribution systems for power loss reduction and voltage profile improvement.

Several advanced optimization techniques have been developed to address the challenges of integrating distributed generation into distribution networks. The Hybrid PIPSO-

SQP Algorithm has been proposed for real power loss minimization in radial distribution systems with optimal distributed generators placement [25]. Similarly, the Improved Northern Goshawk Optimization Algorithm effectively configures renewable energy distributed generators while considering load and generation uncertainties [26]. For comparative analysis, various particle swarm optimization and Differential Evolution algorithms have been utilized for the optimal placement of distributed generators in radial distribution systems [27]. The Bat Algorithm has also been employed for the allocation of solar-based distributed generators to enhance network performance [28]. A combined approach involving gridable electric vehicles and dispersed generation has been designed to further minimize power losses in distribution networks [29]. Additionally, an improved Golden Jackal Optimization Algorithm has been introduced for simultaneous integration of multiple capacitors and multi-type distributed generators, addressing single and multi-objective optimization problems [30]. The Boosting Prairie Dog Optimizer has demonstrated its efficacy in planning wind and solar distributed generators under various dynamic load models [31]. A novel heuristic approach has been developed for the optimal allocation of active and reactive power, improving overall network efficiency [32]. The study by [33] employed the Improved Multi-Objective Function and Info Optimization Algorithm for optimal allocation of distributed generation and distribution static compensator. Finally, the Imperialist Competitive Algorithm and ETAP software using for optimal integration of PV-based distributed denerators and shunt capacitors for 69 bus system [34]. To provide a clearer overview of the existing methods, Table 1 categorizes previous studies based on their datasets and techniques.

Numerous methods have been proposed, ranging from conventional analytical techniques to advanced heuristic and metaheuristic algorithms. However, existing studies often fail to comprehensively address research gaps, such as computational complexity, scalability, and adaptability to real-world constraints. Lack of integrated approaches combining distributed generator and shunt capacitors optimization for real-world networks. Some research gaps can be identified as Insufficient emphasis on computational efficiency and real-time applicability and limited studies addressing practical constraints such as thermal line limits and varying load profiles.

This document develops and applies the optimization technique to determine the optimal locations and sizes of the distributed generator (PV) and Shunt capacitors for various load scenarios, evaluating the performance of the proposed methods. Additionally, we conduct simulations on a distribution system, specifically the IEEE 33-bus and IEEE 69-bus networks, to demonstrate its effectiveness. A comparison of the results obtained with those of other existing techniques proved the superiority of the proposed methods in terms of reducing power losses and improving the voltage profile. The authors made a significant contribution to this document as the first researchers to work on the real ADRAR network and, more importantly, by obtaining good verification results for the objective function in our simulation study after using the improved method Cheetah Optimizer (CO).

The main contributions of this paper are summarized as followed: The Cheetah Optimizer method is applied to the IEEE 33-Bus and IEEE 69-Bus distribution networks, as well as ADRAR distribution network, with the integration of shunt capacities, minimizing power losses and improving the voltage profile; the variation of the load comparing the results obtained with those of the basic case and the insertion of distributed generations with a power factor equal to one.

Table 1. Summary of previous methods for distributed generator and shunt capacitors optimization.

Ref.	IEEE test system	Objective function	Optimization method
[4]	23, 34 and 38 bus radial distribution	Optimal size and power factor of DG unit	(DIAA)
[5]	16, 33 and 69 bus radial distribution	power loss, voltage deviation index	(EOA)
[6]	33 bus radial distribution	power loss, reliability index, reconfiguration	(EOA)
[7]	69 and 119 bus distribution systems	Optimal DG placement, reduce real power loss	(COA)
[8]	33 and 69 bus test systems	Optimal locations and size of the DG, minimizing the power distribution loss.	(PSO)
[9]	33 and 69 bus radial network	Reconfiguration, voltage stability index in the distributed generation (DG)	(MILP)
[10]	33 bus test systems	DG location and sizing and network reconfiguration.	(SPEA2)
[11]	33 and 69 bus distribution systems	Reconfiguration, optimal locations and size of the DG	(ISCA)
[12]	33 and 69 bus distribution systems	Optimal network reconfiguration, optimal integration of DG	(MPSO)
[13]	69 bus distribution systems	Optimal allocation of DSTATCOM, DG and maximize power loss reduction	(ICAO)
[14]	33 bus distribution systems	Optimal DG placement, power loss sensitivity factor (PLSF)	(ROA)
[15]	33 and 69 bus, Tunisian Distribution system.	DG placement and sizing to reduce power loss and improve the voltage profile	(MOPSO)
[16]	33 and 69 bus distribution systems	RDG/BESS/EVCS placement and sizing to reduce power loss	(SMA)
[17]	33 and 69 bus distribution systems	Network reconfiguration and DG allocation problem	(SSA)
[18]	69 and 85 bus East Delta Network Egyptian network	Optimal allocation of shunt capacitors, voltage loss sensitivity factor (VLSF) and reactive power loss sensitivity factor (QLSF) in radial distribution networks	(COA)
[19]	33 and 69 bus distribution systems	Capacitor sizes and their optimal placements	(GA-PSO)
[20]	33 and 69 bus distribution systems	Reducing power loss, and operating costs, improving voltage profiles, and enhancing stability	(CFPSO)
[21]	34 and 85 bus radial distribution systems	Optimal placement of capacitors	(BIOA)
[22]	33 and 94 bus Portuguese distribution systems	Optimal capacitor allocation, maximize the voltage stability, minimize the power losses	(MOCQA)
[23]	16 and 33 bus in distribution grids	Capacitor placement and network reconfiguration	(MICO)
[24]	34 and 85 bus East Delta Network Egyptian network	Optimal capacitor placement, power loss reduction and voltage profile improvement	(HO)
[25]	33, 69 and 118 bus in radial distribution systems	Real Power Loss Minimization, Optimal Placement of DG	PIPSO-SQP
[26]	33 and 69 bus distribution systems	Optimal DG location, capacity, and power factor to minimize energy losses and voltage deviations	(INGO)
[27]	33 and 69 bus distribution systems	Minimize real power losses, injected power from DG	(DE-PSO)
[28]	33 bus distribution systems	Minimize power loss of radial distribution system.	(BA)
[29]	Real network distribution systems	Optimal size of EVs and DGs, reduced power loss and improved voltage profile	(EGOA)
[30]	69 and 118 bus in radial distribution systems	Enhance the voltage profiles, boost stability, and minimize the total active power loss	(GJOA)
[31]	33 bus distribution systems with dynamic load models	Optimal size of PV and WT, reduced power loss and improved voltage profile	(BPDO)
[32]	33, 69 and 119 bus in distribution systems	Optimal allocation of DG and capacitor banks.	(NHA)

The following section describes the problem formulation. The third section concerns cheetah optimization. The results and discussion section are described in section four. Section five is dedicated to the conclusion.

2. PROBLEM FORMULATION

2.1. Load Flow using Forward/ Backward Sweep

Radial distribution networks have certain challenging characteristics, including distributed generation, radial meshed grids, and high R/X ratios. These factors lead to failure of the Newton-Raphson, Gauss-Seidel, and other convergent load flow algorithms with the distribution networks [18]. Thus, this paper analyzes the power flow in the tested distribution networks using an innovative technique termed backward/forward sweep [35]. We layer the network in several directions, starting from the source node. The computation for the forward sweep starts from the source node and proceeds to the designated branch. The computation of the backward sweep begins from the last sorted node and continues back to the source node [18]. Fig. 1 illustrates the power flow equations for radial distribution networks.

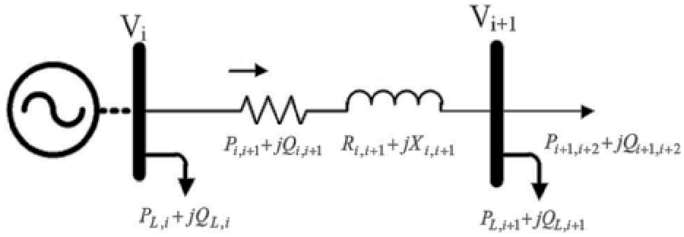

Fig. 1. Single line diagram of the radial distribution system.

The power balance equation must be satisfied [34] :

$$\sum_{i=1}^{n} P_{G,i} = \sum_{i=1}^{n} P_{load,i} + \sum_{i=1}^{n} P_{loss,i} \tag{1}$$

$$\sum_{i=1}^{n} Q_{G,i} = \sum_{i=1}^{n} Q_{load,i} + \sum_{i=1}^{n} Q_{loss,i} \tag{2}$$

where, P_{Gi} and Q_{Gi} are power generations of generators at bus i. P_{Di} and Q_{Di} are the loads at bus i. $P_{loss,i}$ and $Q_{loss,i}$ are the active and reactive power losses.

Between lines i and i + 1, the active and reactive power losses of the ith line are provided as [18]:

$$P_{loss(i,i+1)} = R_{i,i+1}\left(\frac{P_{i,i+1}^2+Q_{i,i+1}^2}{|V_i|^2}\right) \tag{3}$$

$$Q_{loss(i,i+1)} = X_{i,i+1}\left(\frac{P_{i,i+1}^2+Q_{i,i+1}^2}{|V_i|^2}\right) \tag{4}$$

The total active loss can be determined by utilizing Eq. (5):

$$P_{Tloss} = \sum_{i=1}^{n-1} P_{loss(i+1)} = \sum_{i=1}^{n-1}\left(I_{(i+1)}\right)^2 R_i \tag{5}$$

The total reactive loss can be determined by utilizing Eq. (6):

$$Q_{Tloss} = \sum_{i=1}^{n-1} Q_{loss(i+1)} = \sum_{i=1}^{n-1}\left(I_{(i+1)}\right)^2 X_i \tag{6}$$

where, n is the total number of nodes.

Distribution networks install shunt capacitors to inject reactive power and improve the voltage profile. Substations utilize Distributed Generation to inject active energy into networks, stabilizing the voltage and meeting the load during peak hours.

2.2. Objective Function

In general, adding capacitors to the distribution network can improve the voltage profile while decreasing current flow across the lines. Additionally, integrating distributed generators minimizes energy losses, lowers the cost of power loss, and increases the network's energy efficiency. However, installing capacitors raises the cost of the investment. One of the current study's objectives is to reduce total active and reactive energy losses under various limitations without taking into account the capacitor cost. The objective function is defined by Eq. (7) :

$$Min\ F = Min\ S_{loss} = Min \sum_{i=1}^{n} S_{loss\ i} \tag{7}$$

where, S_{loss} is the total apparent power loss (kVA), where n is the number of branches, and S_{lossi} represents the power loss in branch i (kVA).

$$S_{loss\ i} = R_i * |I_i|^2 + X_i * |I_i|^2 \tag{8}$$

where R_i is the resistance of the network branch (Ohm), X_i is the reactance of the network branch (Ohm), and I_i is the current intensity in branch i (A).

2.3. Constraints

The objective functions mentioned above are subject to the following operational constraints.

2.3.1. Tensions Limits

Each node's bus voltage magnitude must be restricted to its permissible range.

$$V_{min} \leq V_i \leq V_{max} \tag{9}$$

where, V_{min} and V_{max} are the minimum and maximum voltage amplitude values for each bar set, respectively V_{max}=1.05 p.u and V_{min}=0.90 p.u

2.3.2. Current Constraints

$$I_i < I_i^{max} \tag{10}$$

where, I_i^{max} is current permissible for branch i within safe limit of temperature.

2.3.3. Power Distributed Generation Limits

$$P_{DG,min} \leq P_{DG,i} \leq P_{DG,max} \tag{11}$$

where, P_{DGmin} and P_{DGmax} are the minimum and maximum active power that can be consumed by the load.
with,

$P_{DGmin,\ 33\ nodes}$=200 KW and $P_{DGmax,\ 33\ nodes}$ =3.7 MW
$P_{DGmin,\ 69\ nodes}$=200 KW and $P_{DGmax,\ 69\ nodes}$ =3.8 MW
$P_{DGmin,\ Adrar}$=200 KW and $P_{DGmax,\ Adrar}$ =3.84 MW

2.3.4. Distributed Generation Location

$$2 \leq GED_n \leq GED_{n,max} \tag{12}$$

where, GED_n is the location of the GED in node and $GED_{n,max}$ symbolizes the number of nodes that are candidates for DG location.

2.3.5. Shunt Capacitor Limits

$$SC_{min} \leq SC_i \leq SC_{max} \tag{13}$$

where, SC_{min} and SC_{max} are respectively the minimum and maximum capacity of the reactive power produced by the shunt capacitors.
with,

$SC_{min,\ 33\ nodes}$=150 KVAr and $SC_{max,\ 33\ nodes}$ =2.3 MVAr
$SC_{min,\ 69\ nodes}$=150 KVAr and $SC_{max,\ 69\ nodes}$ =2.69 MVAr
$SC_{min,\ 33\ nodes}$=150 KVAr and $SC_{max,\ 33\ nodes}$ =4.32 MVAr

2.3.6. Shunt Capacitor Location

$$2 \leq SC_n \leq SC_{n,max} \tag{14}$$

where, SC_n is the location of the SC in node and $SC_{n,max}$ symbolizes the number of nodes that are candidates for SC location.

3. CHEETAH OPTIMIZATION METHOD

The cheetah (Acinonyx jubatus) is a prominent feline species that is the swiftest terrestrial creature. It inhabits the central regions of Iran and Africa [36]. The cheetah can achieve speeds exceeding 120 kilometers per hour. The cheetahs possess physical attributes such as a lengthy tail, elongated and slender legs, a lightweight body, and a flexible spine, which contribute to their agility and speed. Cheetahs are agile creatures with the ability to move silently and swiftly. They possess distinctive spotted coats and are skilled at hunting. However, these visually-oriented predators are unable to sustain their high-speed movements for extended periods of time. Therefore, the duration of the chase must be shorter than 30 seconds [37].

Furthermore, their velocity decreases significantly from 93 km/h or 58 mph to 23 km/h or 14 mph in just three steps once they have captured the victim. In order to compensate for their observation limitations, cheetahs carefully survey their surroundings from elevated positions such as tiny branches or slopes to locate their prey. In addition, these large felines can seamlessly camouflage themselves among tall and arid vegetation because of their distinctive fur patterns [38]. These predators typically prey on Thomson’s gazelles, impalas, antelopes, hares, birds, rodents, and young offspring of larger herd animals. Initially, the predators approach their prey with a deliberate and stealthy gait, assuming a low and concealed position to minimize detection. They then halt in a concealed location, patiently awaiting the prey's approach. When their prey detects their presence, predators stop their hunting activities. The specified minimum distance is around 60-70 meters or 200-230 feet. However, if effective concealment is not possible, we set the distance at 200 meters or 660 feet. The pursuit time is precisely 60 seconds, with an average distance ranging from 173 meters to 559 meters, or 568 feet to 1834 feet. The cheetah strikes the prey's rump with its forepaw, causing the victim to lose its balance and ultimately bringing it down with considerable force. This causes the prey to attempt to flee [39]. The strong tail of the cheetah aids its agile movements, enabling it to make abrupt turns with ease [38, 40]. In general, it is simpler to hunt animals that stray far from their herds or display less caution [41, 42]. The Cheetah Optimizer algorithm is inspired by the hunting strategies of cheetahs, known for their extraordinary speed, agility, and stealth. These strategies are mathematically formulated to mimic two key behaviors: "sit-and-wait" stealth tactics and high-speed chases. The "sit-and-wait" strategy is modeled through randomization and reduced step sizes, enabling the algorithm to perform localized exploration with precision. This minimizes the risk of alerting prey, analogous to avoiding premature convergence in optimization. The high-speed chase behavior is captured through adaptive step-size updates and leader-follower dynamics, which enhance the algorithm's ability to explore global optima efficiently. These biological strategies are integrated into the Cheetah Optimizer algorithm's search phases, ensuring a balance between exploration and exploitation.

3.1. Mathematical Model and Algorithm

During the cheetah's survey of its environment, it can perceive potential prey. Upon spotting its prey, the cheetah may assume a stationary position and patiently await the prey's approach before initiating its assault. The attack mode consists of two phases: rushing and capturing. The cheetah may cease hunting for various reasons, including its limited energy reserves and the rapid movement of its prey. After ten days, the cheetah may return home to rest and prepare for another hunting expedition. The cheetah may select one of these techniques [43] by evaluating the prey, its condition, the surrounding region, and the distance to the prey. In essence, the Cheetah optimizer algorithm relies on the strategic use of different hunting methods during hunting intervals (iterations).

3.1.1. Search Strategy

Cheetahs engage in searching activities, such as scanning and active seeking, within their territory (search space) or the surrounding vicinity, in order to locate their prey. To mathematically represent the seeking strategy of cheetahs, we use the variable $X_{i,j}^{t}$ to indicate the current location of cheetah i (where i ranges from 1 to n) in arrangement j (where j ranges from 1 to D). Here, n represents the number of cheetahs in the population, and D represents the dimension of the optimization issue [44].

The proposed equation for updating the position of Cheetah I in each arrangement is a random search (Eq. 15). It takes into account the cheetah's current position and an arbitrary step size.

$$X_{i,j}^{t+1} = X_{i,j}^{t} + \hat{r}_{i,j}^{-1} . \propto_{i,j}^{t} \tag{15}$$

The variables $X_{i,j}^{t+1}$ and $X_{i,j}^{t}$ represent the next and current places, respectively, of cheetah i in arrangement *j*. The index t represents the current duration of hunting, whereas T represents the maximum duration of hunting. The parameters $\hat{r}_{i,j}^{-1}$ and $\propto_{i,j}^{t}$ are used to control the randomization and step length for cheetah i in arrangement *j*. The second word refers to the randomization term, which involves the use of normally distributed random numbers from a normal distribution, denoted as $\hat{r}_{i,j}$. The step length $\alpha t_{i,j}$, typically more than zero for most applications, can be set as *0.001 × t/T*. This is because cheetahs are known to be slow-walking searchers [44]. Fig. 2a, illustrates the search strategy.

3.1.2. Sit-and-Wait Strategy

While in search mode, the prey may become visible within the cheetah's field of view. In this scenario, any motion made by the cheetah has the potential to alert the prey to its presence, potentially resulting in the prey's escape. To address this issue, the cheetah may opt to employ an ambush strategy, which involves positioning itself on the ground or concealing itself amid the foliage, to approach the prey at close proximity. Thus, in this state, the cheetah remains stationary and patiently awaits the approach of its prey, Fig. 2b. This behavior can be represented or simulated in the following manner [44]:

$$X_{i,j}^{t+1} = X_{i,j}^{t} \tag{16}$$

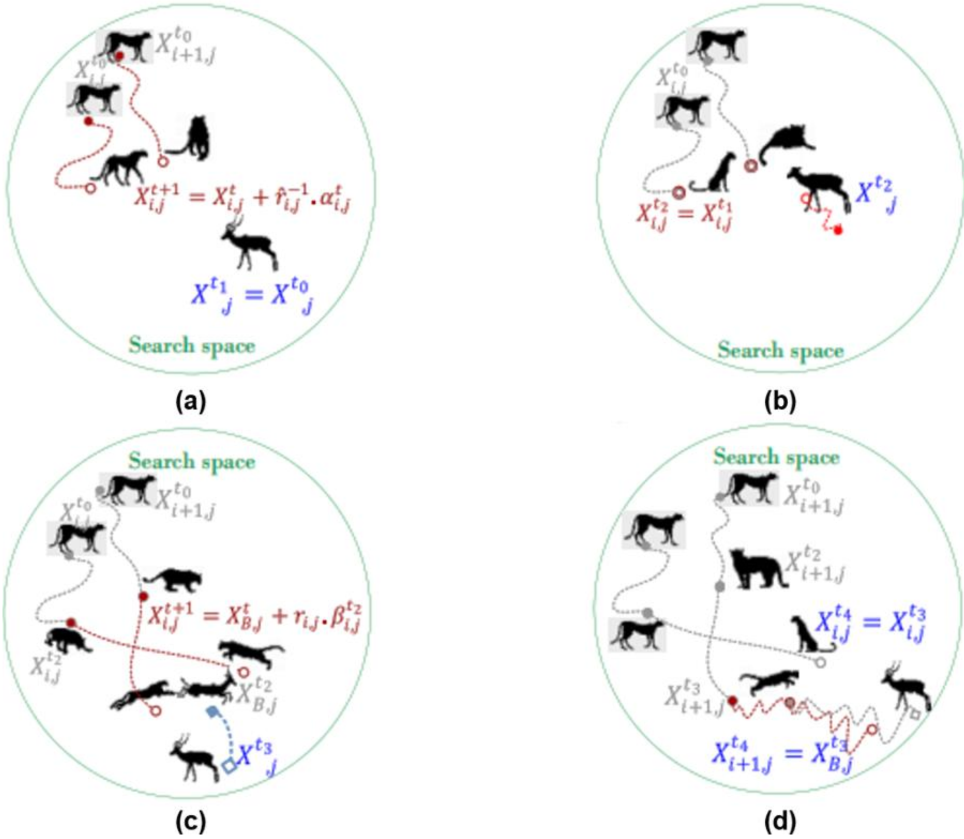

Fig. 2. Graphical representation of Cheetah optimizer strategies [32].

The variables $X_{i,j}^{t+1}$ and $X_{i,j}^{t}$ represent the updated and current positions, respectively, of cheetah i in arrangement j. This technique necessitates that the Cheetah optimizer algorithm refrain from altering all cheetahs concurrently within each group. By doing so, it enhances the likelihood of successful hunting (finding a superior solution) and hence aids in avoiding early convergence.

3.1.3. Attack Strategy

Cheetahs employ two essential factors, speed and flexibility, to launch an attack on their prey. When a cheetah chooses to initiate a chase, it rapidly accelerates towards its prey at top speed. Eventually, the victim becomes aware of the cheetah's assault and starts to flee. The cheetah swiftly chases its victim along the interception path, relying on its sharp eyesight, as depicted in Fig. 2c. Put simply, the cheetah tracks the prey's position and alters its direction of movement to intercept the prey's path at a specific location. Due to the cheetah's ability to reach high speeds over short distances, the prey must quickly alter its location in order to survive. This is illustrated in Fig. 2d, where the cheetah's next position is close to the prey's previous position. Furthermore, as depicted in Fig. 2d, it is likely that one cheetah does not engage in an attack strategy that aligns with the typical hunting behavior of cheetahs. The cheetah utilizes its speed and agility to capture its prey during this phase. During group hunting, individual cheetahs may modify their positions in response to the location of the prey and the leader or nearby cheetahs. In essence, the many methods of hunting employed by cheetahs may be precisely described using mathematical definitions [44]:

$$X_{i,j}^{t+1} = X_{B,j}^{t} + \hat{r}_{i,j}^{-1} . \beta_{i,j}^{t} \tag{17}$$

The variable $X_{B,j}^{t}$ represents the current position of the prey in arrangement j. Put simply, it refers to the present optimal state of the population. The variables $\hat{r}_{i,j}^{-1}$ and $\beta_{i,j}^{t}$ represent the turning factor and interaction factor, respectively, for the cheetah *i* in arrangement j. The reason why $X_{B,j}^{t}$ is employed in Eq (17) is because, during an offensive maneuver, cheetahs employ a high-speed rushing tactic to swiftly approach the prey's location. Therefore, this work computes the updated location of the i-th cheetah in attack mode, taking into account the current position of the prey [44, 45]. In the second term, the turning factor represents the interaction between cheetahs or between a cheetah and a leader during the capturing mode.$\beta_{i,j}^{t}$ Mathematically, this component can be defined as the subtraction of the neighborhood cheetah's location, $X_{k,j}^{t}$ (where k ≠ i), from the i-th cheetah's position, $X_{B,j}^{t}$.

The turning factor $\hat{r}_{i,j}$ in this paper is a random number that is equal to the $|r_{i,j}|^{\exp(\frac{r_{i,j}}{2})}\sin(2\pi r_{i,j})$.

The values of $r_{i,j}$ are generated using a conventional normal distribution, which follows a normal distribution. This element reflects the agile maneuvers of cheetahs when they are in pursuit of prey [42].

The Cheetah Optimizer algorithm shown in Algorithm 1 [44] distinguishes itself from existing metaheuristic approaches through several innovative features. First, the algorithm introduces a dual-phase hunting mechanism combining random exploratory moves and targeted pursuit, which enhances its capability to navigate multi-modal optimization landscapes. Second, its adaptive parameter tuning mechanism dynamically adjusts the randomization factor and step length based on the iteration count, ensuring optimal convergence rates. Furthermore, the incorporation of "sit and wait" and "attack" strategies prevents stagnation by resetting solutions that fail to improve over a defined period, addressing the issue of premature convergence effectively.

4. SIMULATIONS AND DISCUSSION

4.1. Tests Systems

To validate the cheetah optimization, the method has been applied to three test systems:

- IEEE 33-bus standard radial distribution
- IEEE 69-bus standard radial distribution
- ADRAR distribution network (South of Algeria).

All distribution networks are evaluated in various scenarios to achieve the defined objective function of this study. In the simulation part, there are three cases to study for the IEEE 33-Bus, IEEE 69-bus and Adrar distribution network:

- Case I : system includes shunt capacitors
- Case II : optimal integration of Shunt capacitors/ distributed generators with simultaneous load variation
- Case III : optimal integration of distributed generators units with an unity power factor.

Algorithm 1. The Cheetah optimization.

Define th problem data, dimension (D), and the initial population size (n)

Generate the initial population of cheetahs X_i (i=1,2…. n) and evaluate the fitness of each cheetah

Initialize the population's home, leader and prey solutions

t ← 0

it ← 1

MaxIt ← desired maximum number of tierations

T← 60 X[D/10]

while it ≤ MaxIt do

Select m ($2 \leq m \leq n$) members of cheetahs randomly

for each member i ∈ m do

Define the neighbor agent of member i

for each arbitrary arrangement j∈ {1,2…. D} do

Calculate $[\hat{r}, \check{r}, \propto, \beta, H]$

r_2, r_3 ←random numbers are chosen uniformly from 0 to 1

if $r_2 \leq r_3$ then

r_4 ← a random number is chosen uniformly from 0 to 3

if H≥ r_4 then

Calculate new position of member I in arrangement j using Eq. (17)

else

Calculate new position of member I in arrangement j using Eq. (15)

end if

else

Calculate new position of member I in arrangement j using Eq. (16)

end if

end for

Update the solutions of member I and the leader

end for

t←t+1

if t >rand X T and the leader position doesn't change for a time, then

Implement the leave the prey and go back home strategy and change the leader position

Substitute the position of member I by the prey position

t ← 0

end if

it← it +1

Update the prey (global best) solution

end while

These different examples show how the best placement and size of capacitor shunts and distributed generation units can change the parameters of a distribution network, such as power losses and voltage profiles. Furthermore, the implementation of the proposed method Cheetah optimizer should enable a comparison of the findings of the current project with previously published results in the relevant literature. This study uses forward/backward Ssweep [35] to address the OPF problem. To ensure the robustness and efficiency of the Cheetah Optimizer (CO), a sensitivity analysis was conducted on the IEEE 33-bus and IEEE 69-bus systems. The analysis involved varying two key parameters—the step length (α) and the randomization factor (r)—within predefined ranges to evaluate their impact on convergence speed, solution accuracy, and computational time. Since the cheetah is known as a slow walker, the step size was initialized with a small value, and an adaptive epsilon was added to refine the search process as iterations progressed. This adaptive approach ensures a gradual transition from global exploration to local exploitation, enhancing the algorithm's ability to locate optimal solutions without premature convergence. The results, summarized in Table 2, show that varying α, the population size (n), the number of Cheetahs (m), and the maximum number of iterations (Maxiter) directly influences the trade-off between computational efficiency and solution quality. Notably, when α=0.0005 (Case 3), the CO algorithm achieved the lowest power loss (121.10 kW) but required significantly more computational time (24.28 s) due to increased exploitation. Conversely, a higher α (e.g., 0.022 in Case 6) reduced computational time (325.17 s) but resulted in a higher power loss (155.3 kW), indicating reduced solution accuracy. These findings confirm that the step size directly affects the balance between search diversification and convergence speed.

Table 2. Algorithm's performance under varying parameter settings.

Parameter	α	n	m	Maxiter	Time [s]	P_{loss} [kW]	P_{DG} [kW]
1	0.0097	5	3	10	1.42	195.98	7097.6
2	0.0087	10	5	20	4.43	168.72	5727.7
3	0.0005	20	10	30	24.28	121.10	1213
4	0.0167	40	15	40	94.74	117.11	3564.3
5	0.0153	50	20	50	1853.62	108.76	3169.2
6	0.022	55	25	60	325.17	155.3	4755
7	0.0023	60	30	70	512.99	115.9	1522.5

Additionally, the randomization factor r was modeled using a normal distribution r~N(0,1), ensuring controlled randomness in search behavior. This stochastic element prevents the algorithm from stagnating in local optima while maintaining a structured exploration process. The results indicate that the best trade-off between exploration and exploitation was achieved with moderate values of α and r following a Normal distribution, which led to faster convergence and improved optimization performance across all tested cases.

Based on these insights, Table 2 presents the final parameter configurations chosen for all test systems (IEEE-33 bus, IEEE-69 bus, and ADRAR). The optimized values n=50, m=20, and Maxiter=50 provided the best balance between computational efficiency and solution accuracy, ensuring effective performance under different network conditions. These findings highlight the importance of adaptive parameter tuning in metaheuristic optimization, reinforcing the CO algorithm's applicability to real-world power distribution networks.

The Cheetah optimizer parameters in this simulation study are established as outlined in Table 3.

Table 3. Cheetah optimizer parameters for three tests systems.

Parameter	Test system		
	IEEE-33 BUS	IEEE-69 BUS	ADRAR
Number of populations	n = 50	n = 50	n = 50
Maximum iterations	Max_iter = 50	Max_iter = 50	Max_iter = 50
Number of search agents	m = 20	m = 20	m = 20

4.2. Results and Discussion for IEEE 33-Bus Radial Distribution Networks

The IEEE small-scale radial distribution networks standard, which has 32 branches and 33 buses, is the first test network. A single-line diagram of the tiny DS is shown in Fig. 3. Total reactive and active loads at nominal load are 2.3 MVAr and 3.715 MW, respectively, at 12.66 kV and 100 MVA base values. The load and line data for the test network are given in [43]. The findings of the tide calculation at nominal load indicate that the system without distributed generators and shunt capacitors installation has a reactive network loss of 143.13 kVAr and an active network loss of 211 kW. Bus 18 has the lowest voltage magnitude of 0.9038 p.u, and a voltage deviation of 0.1338 p.u.

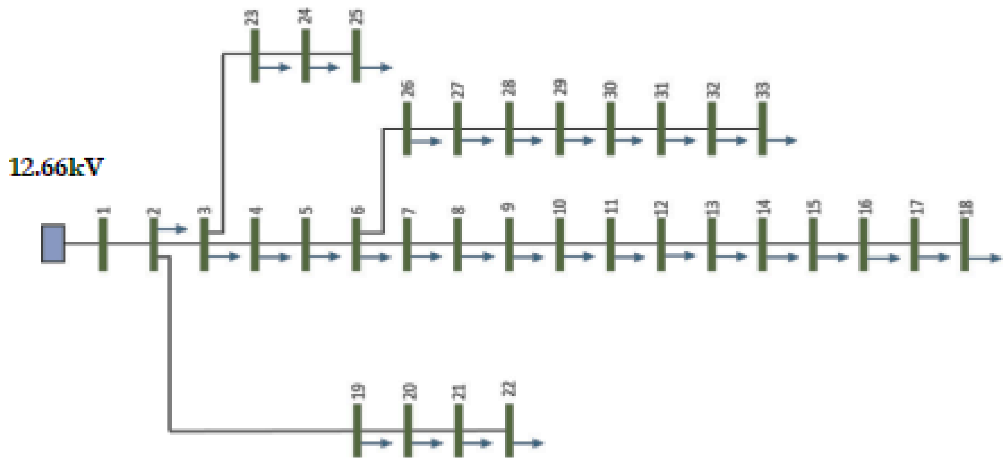

Fig. 3. IEEE 33-Bus radial distribution system.

4.2.1. Case I : Optimal Integration of Shunt Capacitors

The results in Table 4 show the positive effect of adding shunt capacitors to reduce active losses in a 33-node distribution network. The addition of a single shunt capacitor of 1391 kVAr reduces active losses to 145.54 kW, which is a decrease of 31.03% compared to the base case.

Table 4. Comparison of optimal results obtained by Cheetah optimizer and Cf-PSO for a 33-node network.

	Base case	1 SC	2 SCs	3S Cs	4 SCs
SC size [kVAr] Bus [20]	/	1266 30	465, 1035 12, 30	388, 544, 1037 13, 24, 30	431, 301, 432, 1035 7, 14, 24, 30
SC size [kVAr] Bus [CO]	/	1391 29	458.7, 1013.8 12, 30	359.1, 533.4, 1012 13, 23, 30	416.4, 327, 462.1, 1062.6 6, 12, 24, 30
P_{loss} (kW) [20]	211	151.40	141.86	138.28	136.85
P_{loss} (kW) [CO]	211	145.54	135.84	133.13	132.2
RP_{loss} (%) [20]	/	28.24	32.78	34.46	35.15
RP_{loss} (%) [CO]	/	31.03	35.62	36.90	37.34
Q_{loss} (kVAr) [20]	143.13	103.91	96.49	94.28	93.78
Q_{loss} (kVAr) [CO]	143.13	97.77	90.57	89.08	88.49
V_{min} (p.u) Bus [20]	0.9038 /	0.9165 /	0.9303 /	0.9317 /	0.9340 /
V_{min} (p.u) Bus [CO]	0.9131 18	0.9268 18	0.9356 18	0.9368 18	0.9374 17

By adding two shunt capacitors of 458.7 kVAr and 1013.8 kVAr, the active losses drop to 135.84 kW, representing a reduction of 35.62%. Compared to the first case, this configuration is more efficient, suggesting that the positioning and distribution of shunt capacitors play a role in optimizing losses. With three shunt capacitors of 359.1 kVAr, 533.4 kVAr, and 1012 kVAr, the active losses are reduced to 133.13 kW, corresponding to a decrease of 36.90%. The addition of shunt capacities continues to reduce active losses. The insertion of four shunt capacitors of 416.4 kVAr, 327 kVAr, 462.1 kVAr, and 1062.6 kVAr reduces active losses to 132.2 kW, representing a reduction of 37.34%. This configuration shows the best reduction among the tested cases. These results illustrate that increasing the number of shunt capacitors and optimizing their distribution allows for a gradual reduction in active losses. Fig. 4, demonstrates the voltage profiles of IEEE 33-bus. The voltage profile improves as the number of SCs increases. The insertion of shunt capacitors increases the minimum voltage from 0.9131 p.u to 0.9374 p.u, resulting in improved voltage stability.

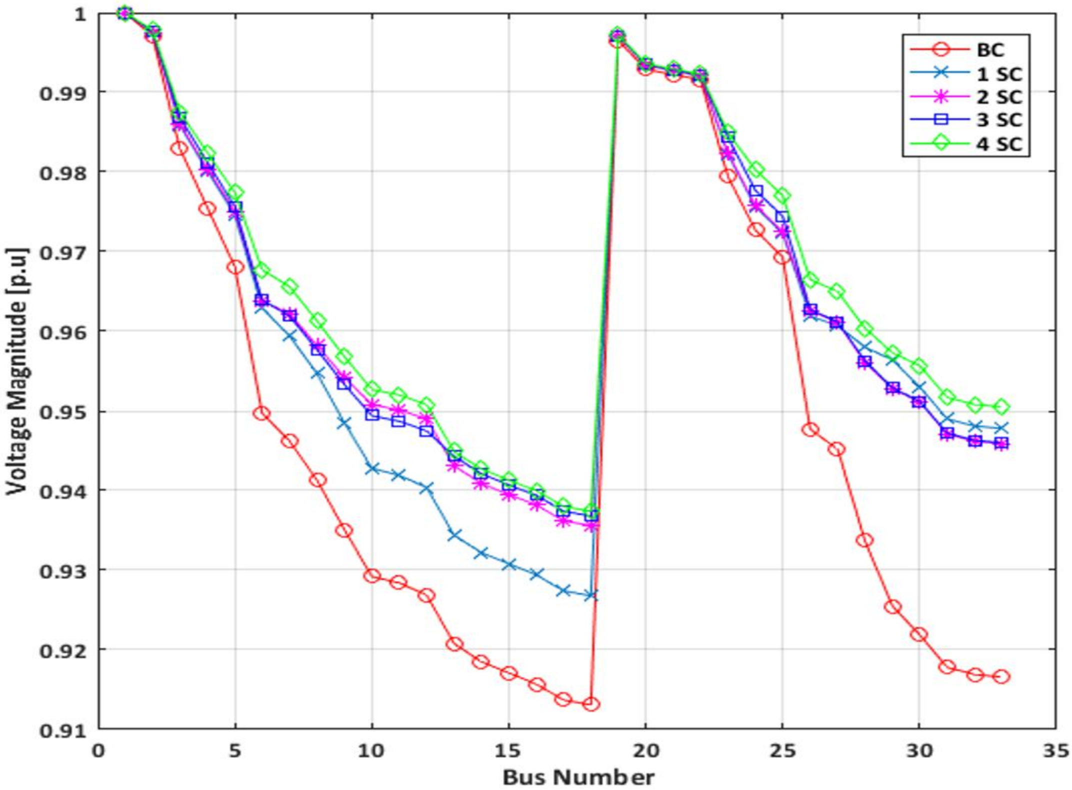

Fig. 4. Voltage distribution in the 33-bus system for different cases.

The proposed Cheetah optimizer method, aimed at minimizing power losses, is objectively compared to the results in recent literature and to the case studies presented in Table 4 for the IEEE 33-bus distribution network.

The proposed Cheetah optimizer was validated against established techniques such as the Bat Algorithm, moth flame optimization algorithm hybrid sine cosine algorithm, the bacterial foraging optimization, flower pollination algorithm, cuckoo search algorithm and the Highly Effective Algorithm (MSFS), among others. In the majority of instances, the reduction in the percentage of power loss observed by the Cheetah optimizer in Table 5 exceeds that of existing techniques.

Figs. 5a and 5b compare the active and reactive power loss across all four scenarios.

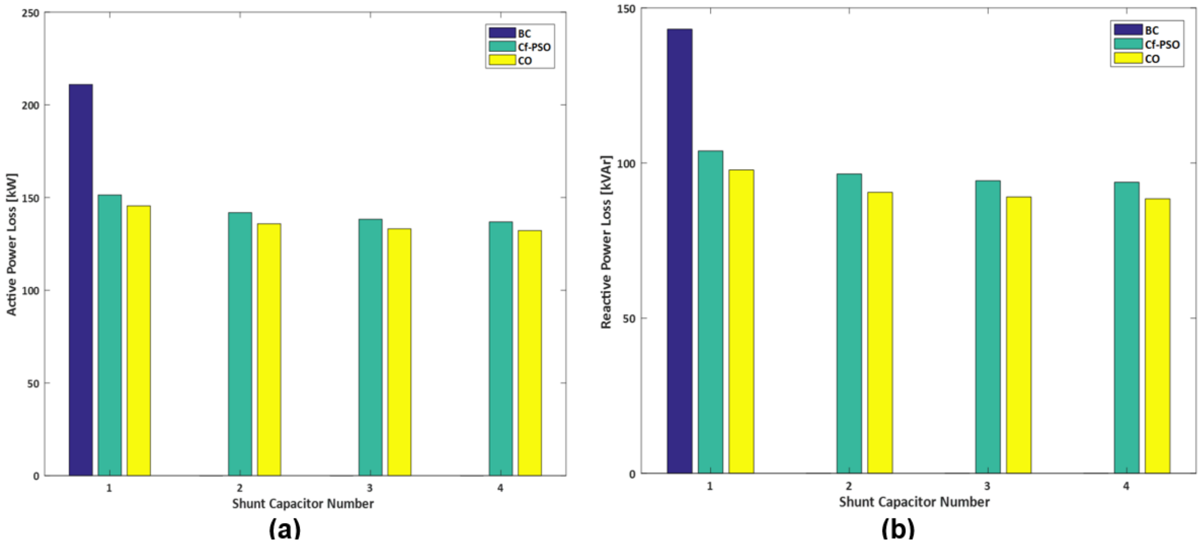

Fig. 5. Comparison of power loss for 33-bus IEEE: a) active power loss; b) reactive power loss.

Table 5. Comparison of power losses with different methods for three cases of the 33-bus system.

Case	Method	SC size (kVAr)	Location Bus	P_{loss} [kW]	P_{loss} [%]
Base case		/	/	211	/
Case one 1 SC	Analytical [46]	1000	33	164.60	22.83
	BA [47]	1800	30	161.48	23.86
	MFO-SCA [48]	1258	30	151.37	28.26
	CSA [49]	1200	30	151.52	28.18
	PSO [20]	1649	29	156.57	24.46
	CF-PSO [20]	1266	30	151.40	28.25
	CO (proposed)	1391	29	145.54	31.03
Case two 2 SCs	Analytical [46]	850, 860	7, 29	146.64	30.50
	WIPSO-GSA[50]	470, 1060	12, 30	141.84	32.77
	CSA [49]	1000, 400	30, 13	142.07	32.66
	SCA [51]	350, 1000	14, 30	142.55	32.44
	MFO-SCA [48]	465, 1063	12, 30	141.84	32.77
	PSO [20]	465, 1063	12, 30	141.86	32.78
	CF-PSO [20]	465, 1035	12, 30	141.86	32.78
	NCB-HM [32]	405, 1052	13, 30	141.9	32.74
	HM [52]	430, 1040	12, 30	141.94	32.72
	MSFS [53]	465.2, 1063.3	12, 30	141.843	32.77
	CO (proposed)	458.7, 1013.8	12, 30	135.84	35.62
Case three 3 SCs	BFOA [54]	349.6, 820.6, 277.3	18, 30, 33	144.04	31.73
	CSA [49]	450, 400, 950	11, 24, 30	138.54	34.33
	MFO-SCA [48]	382, 334, 1009	13, 24, 30	138.91	34.16
	PSO [20]	388, 544, 1037	13, 24, 30	138.28	34.47
	CF-PSO [20]	388, 544, 1037	13, 24, 30	138.28	34.47
	FPA [55]	450, 450, 900	13, 24, 30	139.075	34.08
	NCB-HM [32]	383, 386, 1000	13, 25, 30	138.65	34.28
	CPM [56]	500, 500, 1000	12, 24, 30	138.61	34.30
	CPM [57]	359, 520, 1016	13, 24, 30	138.37	34.41
	HM [52]	360, 510, 1020	13, 24, 30	138.37	34.41
	MSFS [53]	436.2, 538.4 1015	12, 24, 30	138.31	34.44
	CO (proposed)	359.1, 533.4, 1012	13, 23, 30	133.13	36.90

4.2.2. Case II : Load Variation with Multiple Distributed Generators

Table 6 presents the performance of the proposed Cheetah optimizer across three different load levels and three distributed generators. Table 6 reveals that the test system's nominal load reduces the base power loss (kW) from 202.68 to 17.45 kW. In the light load scenario, the active loss drops to 17.32 kW from the base power loss of 47.07 kW.

The same observation for the peak load, or Cheetah optimizer, results in power active losses reduced to 190.21 kW, compared to the base case of 575.39 kW. Table 6 presents a comparison between the proposed Cheetah optimizer method and the parameter improved particle swarm optimization hybrid sequential quadratic programming result from the literature to illustrate the performance of the proposed method. The table reveals that at all load levels, the Cheetah optimizer outperforms the parameter Improved Particle Swarm Optimization in terms of loss reduction and voltage profile improvement.

Table 6. Optimization of losses with three levels of load in the presence of three distributed generators in the 33-bus system.

Case	Method	DG size [kW]	Bus location	P_{loss} [kW]	Q_{loss} [kVAR]	V_{min} [p.u]	Bus location
Base case 50%		-	-	47.07	31.35	0.9583	18
Base case 100%		-	-	202.68	135.17	0.9131	18
Base case 160%		-	-	575.39	384.34	0.8528	18
Case one 50% Light	PIPSO-SQP [25]	445.98 504.54 486.08	12 30 24	17.97	12.34	0.9824	18
	CO (proposed)	372.34 532.85 554.21	14 30 24	17.32	31.35	0.9846	33
Case two 100% Nominal	PIPSO-SQP [25]	1053.63 1091.38 801.81	30 24 13	72.78	50.66	0.9687	33
	CO (proposed)	754.9 1104.1 1069	14 24 30	71.45	49.4	0.9686	33
Case three 160% Peak	PIPSO-SQP [25]	1062.58 1233.54 1645.55	14 31 6	208.94	145.26	0.9505	18
	CO (proposed)	1229.5 1801.2 1760.8	14 24 30	190.21	131.65	0.9501	33

Figs. 6 and 7 show the reduction in power losses and the improvement in the voltage profile for the three load conditions, respectively. However, reduction in power losses and improvement in voltage profile for the three load conditions demonstrate the superiority of the proposed Cheetah optimizer. Fig. 7 also shows an improvement in the minimum bus voltage (Vmin) at all load levels (light, nominal, and peak) from 0.9583, 0.9132, and 0.8528 to 0.9846, 0.9686, and 0.9501 p.u. These values respect the voltage constraints.

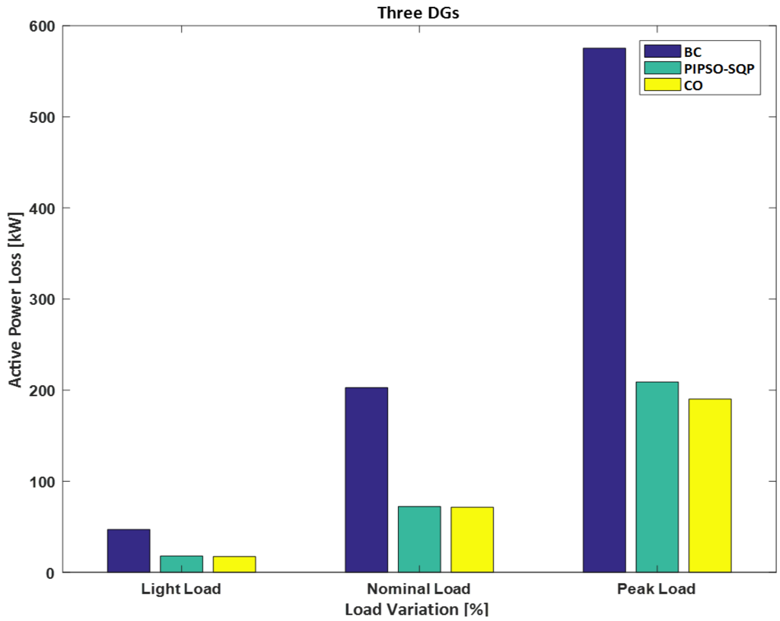

Fig. 6. Comparison of active power loss for different load conditions with three distributed generators.

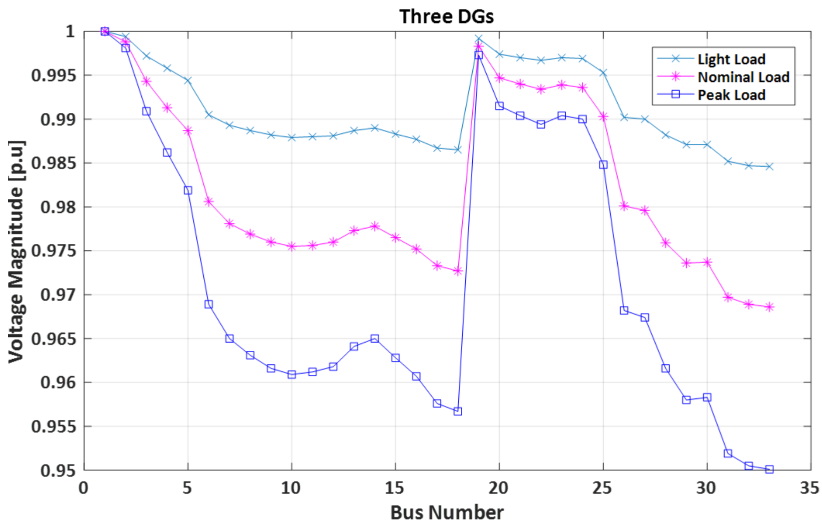

Fig. 7. Voltage distribution in the 33-bus system for various load conditions.

4.2.3. *Case III : Optimal Integration of Distributed Generators with Unity Power Factor*

We assume that the distributed generators in this example contribute only active power to the network and have power factors of 1.0. We use the Cheetah optimizer algorithm to optimize the distributed generator dimensions and positions to minimize active power loss. We obtained detailed information by optimizing the configuration of different distributed generator numbers using the suggested Cheetah Optimizer algorithm, as shown in Table 7. This information comprises the distributed generators location and capacity, the power loss P_{loss} and Q_{loss}, the reduction of active and reactive losses RP_{loss}, and indicators such as the minimum system voltage magnitude. Installing one, two, or three distributed generators reduces active losses for the Cheetah Optimizer method by 48.45%, 59.20%, and 66.11%, and for improved northern goshawk optimization algorithm by 42.9%, 58.2%, and 64.6%, respectively. The more distributed generators in the network increases, the more significant the reduction in losses becomes. Moreover, the integration of distributed generators into the network can also improve the system's voltage profile.

Table 7. Comparison of optimal results obtained by Cheetah optimizer and improved northern goshawk optimization algorithm for a 33-node network at the unity power factor.

	Base case	1 DG	2 DGs	3 DGs
DG size [kW] Bus [26]	/	2590.25 6	851.5, 1157.63 13, 30	1053.7, 1091.37, 801.67 30, 24, 13
DG size [kW] Bus [CO]	/	3169.2 6	1117.6, 907 30, 13	1043.2, 1080.9, 806.8 30, 24, 13
P_{loss} [kW] [26]	211	111.03	87.17	72.79
P_{loss} [kW] [CO]	211	108.76	86.07	71.51
RP_{loss} [%] [26]	/	47.38	58.69	65.5
RP_{loss} [%] [CO]	/	48.45	59.20	66.11
Q_{loss} [kVAr] [26]	143.13	81.71	59.81	50.68
Q_{loss} [kVAr] [CO]	143.13	78.59	58.60	49.40
V_{min} [p.u] Bus [34]	0.9038 18	0.9424 18	0.9685 33	0.9687 33
V_{min} (p.u) Bus [CO]	0.9131 18	0.9593 18	0.9680 33	0.9684 33

Fig. 8 demonstrates the voltage profiles of the IEEE 33 bus system. The voltage profile improves as the number of distributed generators increases. The insertion of the distributed generators increases the minimum voltage from 0.9131 p.u to 0.9684 p.u resulting in improved voltage stability. The effectiveness of Cheetah Optimizer is validated by comparing it with the optimal solutions of improved northern goshawk optimization, northern goshawk optimization, differential evolution and particle swarm optimization (DAPSO), enhanced grasshopper optimization algorithm (EGOA), and bat algorithm, as illustrated in Table 8. When one, two, or three distributed generators are configured in the distribution system, the losses incurred by the Cheetah Optimizer algorithm are inferior to those of the improved northern goshawk optimization, northern goshawk optimization, differential evolution and particle swarm optimization, enhanced grasshopper optimization algorithm, and bat algorithm methodologies, which illustrates the superiority of the Cheetah Optimizer algorithm in addressing the optimal distributed generation allocation problem.

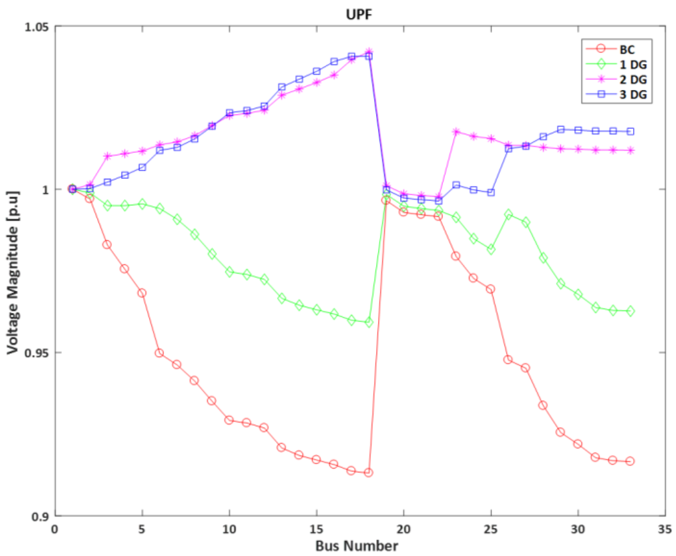

Fig. 8. Voltage distribution in the 33-bus system for different cases

In Figs. 9a and 9b, we can see a comparison of the active and reactive power loss across all three scenarios.

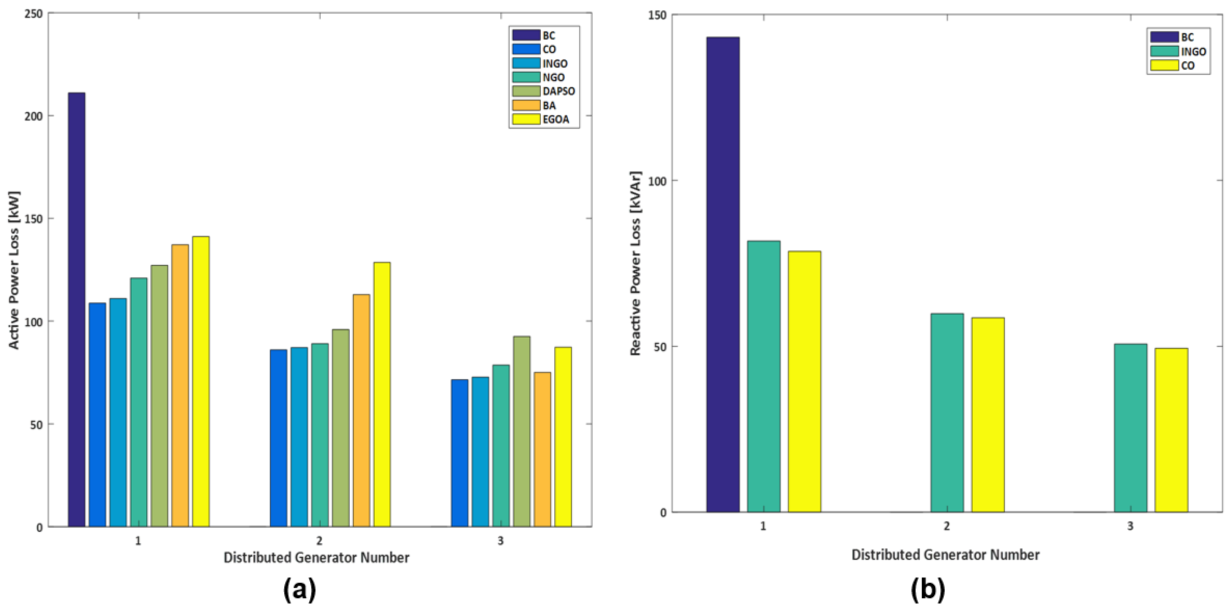

Fig. 9. Comparison of power loss for IEEE 33-bus: a) active power loss; b) reactive power loss.

Table 8. Comparison of the results obtained by the Cheetah optimizer algorithm and other algorithms for the 33-bus system at the unity power factor.

Case	Method	DG size [kW]	Bus location	P_{loss} [kW]	P_{loss} [%]
Base case		-	-	211	-
Case one 1 DG	CO (proposed)	3169.2	6	108.76	48.45
	INGO [26]	2590.25	6	111.03	47.38
	NGO [26]	1695.98	7	120.98	42.66
	DAPSO [27]	1212	8	127.17	39.73
	BA [28]	816.3	15	137.2	34.98
	EGOA [42]	902.9	17	141.12	33.12
Case two 2 DGs	CO (proposed)	1117.6, 907	30, 13	86.07	59.20
	INGO [26]	851.5, 1157.63	13, 30	87.17	58.69
	NGO [26]	1351.23, 804.53	28, 13	89.04	57.8
	DAPSO [27]	1227, 738	13, 32	95.93	54.54
	BA [28]	952.4, 952.4	15, 25	112.88	46.5
	EGOA [29]	962.3, 184.5	17, 18	128.56	39.07
Case three 3 DGs	CO (proposed)	1043.2, 1080.9 806.8	30, 24 13	71.51	66.11
	INGO [26]	1053.7, 1091.37, 801.67	30, 24 13	72.79	65.5
	NGO [26]	995.29, 814.62 1258.84	30, 13 3	78.63	62.73
	DAPSO [27]	681, 600, 719	10, 18 31	92.55	56.14
	BA [28]	816.3, 952.35 952.35	15, 25 30	75.05	64.43
	EGOA [29]	674.81, 171.04 1032.31	17, 18 31	87.31	58.62

4.3. Results and Discussion for IEEE 69-Bus Radial Distribution Networks

The IEEE radial distribution networks standard, which has 68 branches and 69 buses, is the second test network. A single-line diagram is shown in Fig. 10. Total reactive and active loads at nominal load are 2.69 MVAr and 3.8 MW, respectively, at 12.66 kV, and 100 MVA base values.

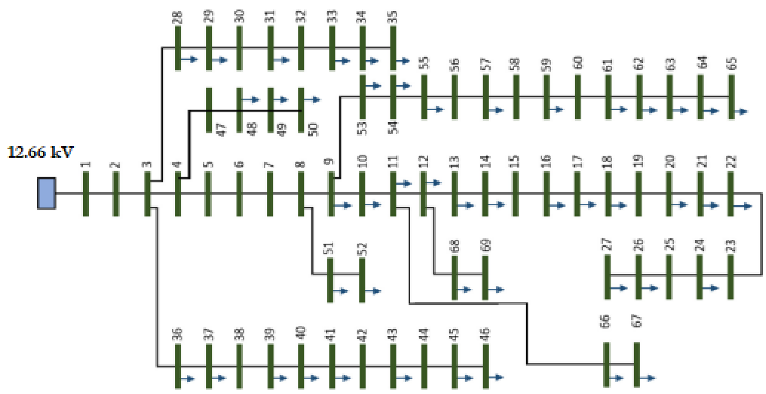

Fig. 10. IEEE 69-Bus radial distribution system.

The test network's load and line data are presented in [25]. The results of the flow calculation at nominal load show that the system without shunt capacitors installation has an active network loss of 225 kW and a reactive network loss of 102.15 kVAr. The bus 67 has the lowest voltage magnitude of 0.9091 p.u.

4.3.1. Case I : Optimal Integration of Shunt Capacitors

In the present scenario, the shunt capacitors only deliver reactive power into the network. The net active power loss achieved by the Cheetah optimizer, improved golden jackal optimization algorithm (IGJO), original golden jackal optimization (GJO), Hybrid MFOSCA,WeevilOA, skill optimization algorithm (SOA) and Tasmanian devil optimization (TDO) is nearly the same for one, two, and three shunt capacitors, i.e., 152.01, 146.421, and 145.11 kW, as shown in Table 9.

Table 9. Comparison with different methods for integration of capacitor banks for the 69 bus system.

Case	Method	SC size [kVAr]	Location Bus	P_{loss} [kW]	P_{loss} [%]	V_{min} [p.u]
Base case	-	-	-	225	-	0.9091
Case one 1 SC	CO (proposed)	1329.90	61	152.01	32.44	0.9307
	IGJO [30]	1329.99	61	152.04	32.44	0.9307
	GJO [30]	1330.00	61	152.04	32.44	0.9307
	WeevilOA [30]	1329.99	61	152.04	32.44	0.9307
	SOA [30]	1329.99	61	125.04	32.44	0.9307
	TDO [30]	1329.99	61	152.04	32.44	0.9307
	Hybrid MFOSCA [48]	1330.00	61	152.04	32.44	-
Case two 2 SCs	CO (proposed)	361.4, 1276.8	17, 61	146.42	34.92	0.9312
	IGJO [30]	361.08, 1275.05	17, 61	146.44	34.91	0.9311
	GJO [30]	360.64, 1275.03	17, 61	146.44	34.91	0.9311
	WeevilOA [30]	361.08, 1275.05	17, 61	146.44	34.91	0.9311
	SOA [30]	361.08, 1275.05	17, 61	146.44	34.91	0.9311
	TDO [30]	361.08, 1275.08	17, 61	146.44	34.91	0.9311
	Hybrid MFOSCA [48]	361, 1275	17, 61	146.44	34.91	-
Case three 3 SCs	CO (proposed)	381.7, 243.8, 1225.7	11, 21, 61	145.11	35.50	0.9313
	IGJO [30]	391.62, 252.24, 1232.41	11, 17, 61	145.12	35.49	0.9314
	GJO [30]	392.87, 252.28, 1231.80	11, 17, 61	145.12	35.49	0.9314
	WeevilOA [30]	384.58, 259.40, 1232.41	11, 15, 61	145.29	35.42	0.9314
	SOA [30]	388.77, 270.94, 1230.03	10, 15, 61	145.34	35.40	0.9314
	TDO [30]	391.31, 252.09, 1232.55	11, 17, 61	145.12	35.498	0.9314
	Hybrid MFOSCA [48]	389, 253, 1253	11, 17, 61	145.12	35.498	-

Nonetheless, the Cheetah optimizer method results in the lowest possible power loss, which is achieved by deploying shunt capacitors. It can be seen that all optimization methods give equal minimum voltage values across diverse scenarios.

Fig. 11 demonstrates the voltage profiles of IEEE 69-bus. The voltage profile improves as the number of shunt capacitors increases. The insertion of shunt capacitors increases the minimum voltage from 0.9091 p.u. to 0.9314 p.u, resulting in improved voltage stability. Fig. 12 compares the active power loss across three scenarios for different algorithms.

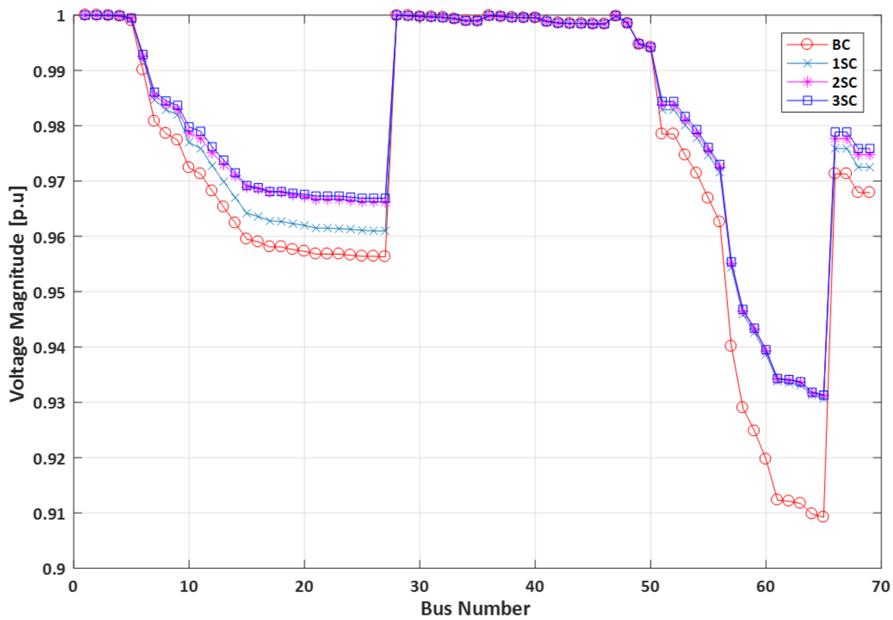

Fig. 11. Voltage distribution in the 69-bus system for different cases.

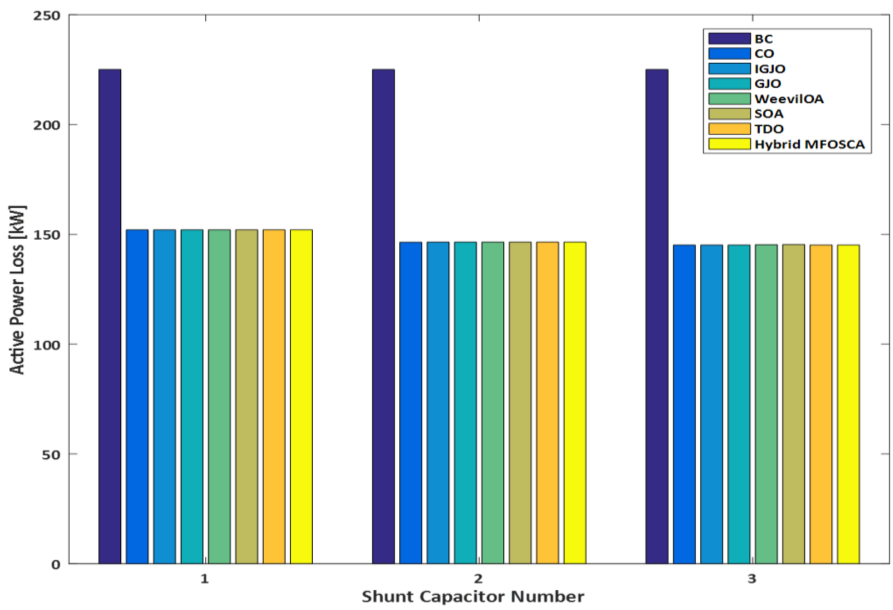

Fig. 12. Comparative active power loss for 69-bus IEEE.

4.3.2. Case II : Load variation with two shunt capacitors

Table 10 presents the performance of the proposed Cheetah optimizer across three different load levels and two shunt capacitors. Table 10 reveals that the test system's case one

(100% load) reduces the base power loss (kW) from 225 to 146.42 kW. In case two (75% load), the active loss drops to 81.55 kW from the base power loss of 121.01 kW. Figs. 13 and 14 show the active power losses and the voltage profile for the three load conditions, respectively.

Table 10. Losses optimization with three load levels in the presence of 2 shunt capacitors s in the 69-bus system.

Case	Method	SC size [kVAr]	Location Bus	P_{loss} [kW]	Q_{loss} [kVAR]	V_{min} [p.u]	Location Bus
Base case 100%		/	/	225	102.15	/	/
Base case 75%		/	/	121.01	55.087	/	/
Base case 50%		/	/	51.59	23.54	/	/
Case one 100%	COA [18]	300 1200	17 61	146.87	/	0.928	/
	CO (proposed)	363.7 1275.1	17 61	146.42	68.22	0.9311	65
Case two 75%	COA [18]	0 900	17 61	83.053	/	0.9459	/
	CO (proposed)	69.40 909.55	18 61	81.55	38.06	0.9484	64
Case three 50%	COA [18]	0 600	17 61	35.757	/	0.9657	/
	CO (proposed)	133.53 671.71	18 61	34.47	16.14	0.9671	65

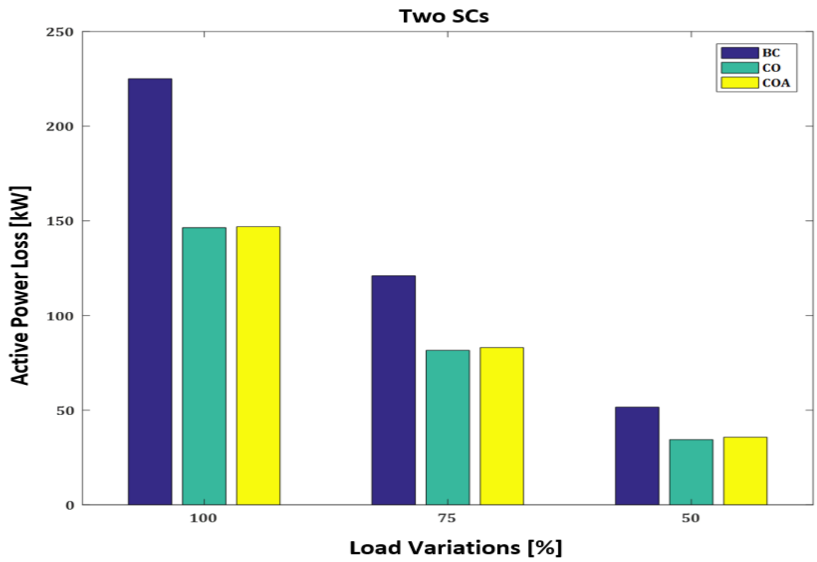

Fig. 13. Comparison of active power loss for different load conditions with two shunt capacitors.

The same observation for case three (50% load), or Cheetah optimizer, results in a reduced value of power active losses of 34.47 kW, compared to the base case of 51.59 kW. To illustrate the performance of the proposed method, Table 9 presents a comparison between the proposed Cheetah optimizer and the combined optimization approach (COA) result from the literature. The table reveals that at all load levels, the Cheetah optimizer outperforms the combined optimization approach in terms of loss reduction and voltage profile improvement.

4.3.3. Case III : optimal integration of distributed generator with unity power factor (UPF)

The Cheetah optimizer algorithm optimizes the position and capacity of one, two, and three units of distributed generators to reduce active power loss.

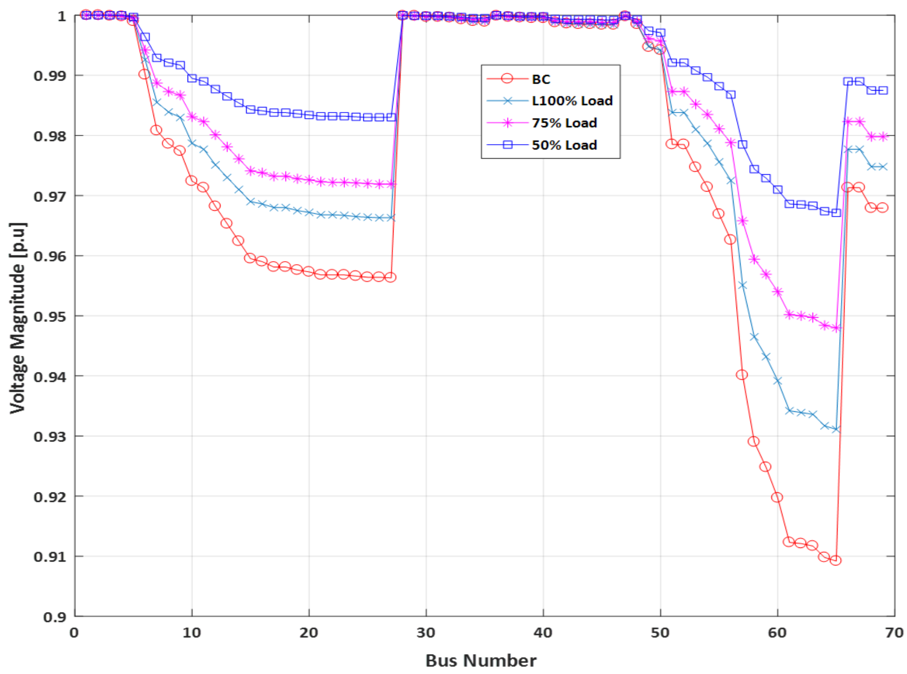

Fig. 14. Voltage distribution in the 69-bus system for different load conditions.

The voltage distribution becomes more uniform, approaching 1 p.u., and the voltage magnitudes of all buses fall within the range specified in this study. This demonstrates that the Cheetah optimizer method remains effective even when dealing with more complex optimization issues. Table 11 displays the full outcomes of using the Cheetah optimizer algorithm to set up 1, 2, and 3 distributed generators in the IEEE 69-bus test system. This shows that a smart distributed generator configuration in the IEEE 69-bus system can significantly lower active power loss. This mirrors the case of what happened in the IEEE 33-bus system simulation: configured distributed generators lower both active and reactive network losses, and raise the minimum voltage. Installing one, two, or three distributed generators lowers active network loss by 63.026%, 68.155%, and 69.268%, respectively. The minimum voltage increases from 0.9092 to 0.9684, and 0.9790.

Table 11. Comparison of optimal results obtained by Cheetah optimizer and improved northern goshawk optimization for a 69-node network at the unity power factor.

	Base case	1 DG	2 DGs	3 DGs
DG size [kW] Bus [30]	-	1872.70 61	531.48, 1781.47 17, 61	526.66, 380.51, 171.97 11, 17, 61
DG size [kW] Bus [CO]	-	1885 61	1782.8, 534.4 61, 17	526.4, 308.2, 1719.1 11, 18, 61
P_{loss} [kW] [30]	225	83.22	71.67	69.42
P_{loss} [kW] [CO]	-	83.19	71.65	69.40
P_{loss} [%] [30]	-	63.01	68.146	69.145
P_{loss} [%] [CO]	225	63.026	68.155	69.268
Q_{loss} [kVAr] [30]	102.15	-	-	-
Q_{loss} [kVAr] [CO]	102.15	40.50	35.92	34.95
V_{min} [p.u] Bus [30]	0.9091 -	0.9683 -	0.9789 /	0.9790 /
V_{min} [p.u] Bus [CO]	0.9092 67	0.9684 27	0.9790 65	0.9790 65

Table 12 compares the simulation results of the Cheetah optimizer method with those of the Improved golden jackal optimization algorithm, original golden jackal optimization, hybrid Moth Flame Optimization and algorithm and Sine Cosine Algorithm, The modified prairie dogs optimizer, and prairie dog optimizer algorithms. This research proposes the Cheetah optimizer approach, which, when used with the same number of distributed generators, results in lower active network loss than previous algorithms. Figs. 15 and 16 show the improvement in the voltage profile for the three conditions and the reduction in power losses, respectively.

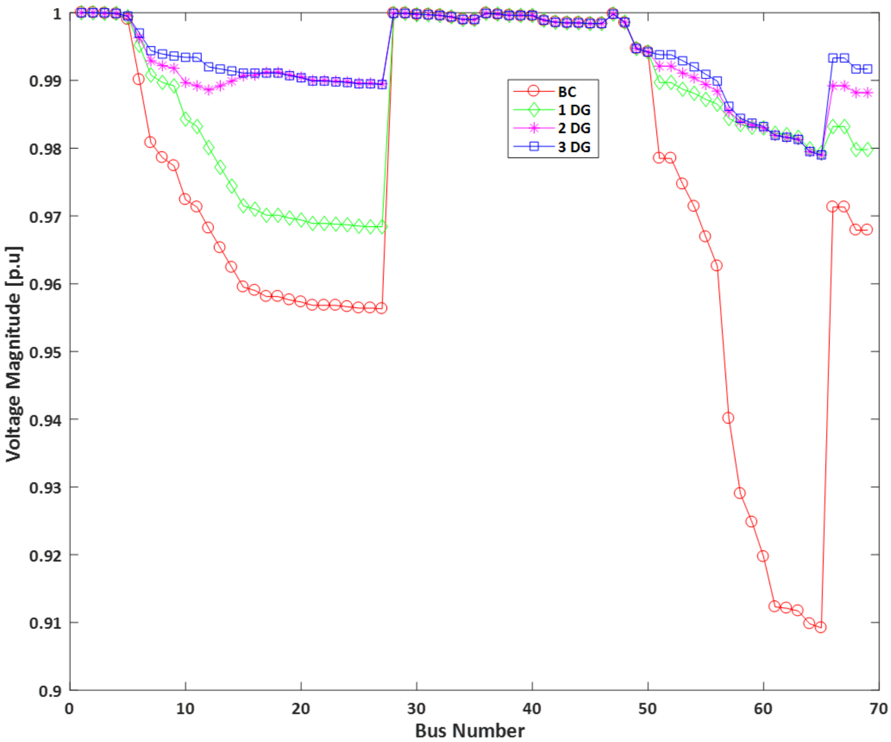

Fig. 15. Voltage distribution in the 69-bus system for different cases.

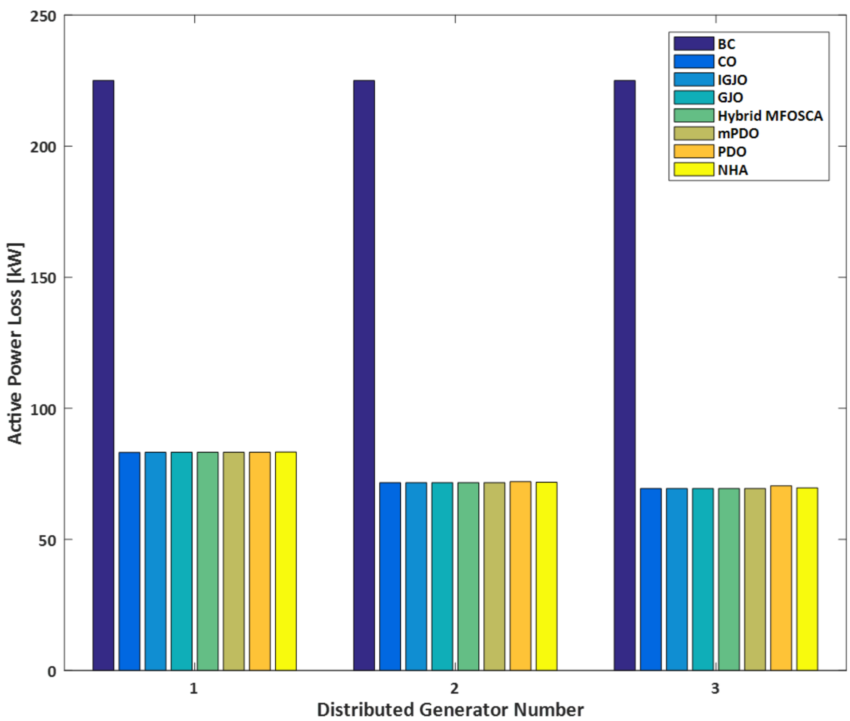

Fig. 16. Comparative active power loss for 69-bus IEEE.

Table 12. Comparison of the results of the Cheetah optimizer algorithm with other algorithms for the 69-bus system at the unity power factor.

Case	Method	DG size [kW]	Location Bus	P_{loss} [kW]	P_{loss} [%]
Base case		/	/	225	/
Case one 1 DG	CO (proposed)	1885	61	83.19	63.026
	IGJO [30]	1872.70	61	83.223	63.012
	GJO [30]	1872.71	61	83.223	63.012
	Hybrid MFOSCA [48]	1872.73	61	83.224	63.012
	mPDO [31]	1872.70	61	83.223	63.012
	PDO [31]	1862.25	61	83.226	63.010
	NHA [32]	1823.00	61	83.30	62.978
Case two 2 DGs	CO (proposed)	1782.8, 534.4	16, 17	71.65	68.155
	IGJO [30]	531.48, 1781.47	17, 61	71.675	68.144
	GJO [30]	531.22, 1782.14	17, 61	71.675	68.144
	Hybrid MFOSCA [48]	531.12, 1781.5	17, 61	71.674	68.144
	mPDO [31]	531.483, 1781.470	17, 61	71.675	68.144
	PDO [31]	457.643, 1732.553	17, 61	72.021	67.990
	NHA [32]	520.00, 1733.00	17, 61	71.80	6.089
Case three 3 DGs	CO (proposed)	526.4, 308.2, 1719.1	11, 18, 61	69.40	69.268
	IGJO [30]	526.66, 380.51, 1718.97	11, 17, 61	69.42	69.14
	GJO [30]	525.52, 380.54, 1719.26	11, 17, 61	69.42	69.14
	Hybrid MFOSCA [48]	526.44, 380.27, 1719.8	11, 17, 61	69.42	69.14
	mPDO [31]	526.668, 380.510, 1718.970	11, 17, 61	69.427	69.143
	PDO [31]	309.420, 306.146, 1785.549	12, 16, 61	70.48	68.673
	NHA [32]	471.00, 312.00, 1689.00	12, 21, 61	69.70	69.022

4.4. Results and Discussion for Real-Word ADRAR Distribution Network

Since the Cheetah optimizer optimization method gives the best results when applied to the two previous test networks ''IEEE 33-bus'' and ''IEEE 69-bus,'' and when compared to previous works, the following study consists of validating the performance of this technique by analyzing its response when applied to a real distribution system such as the ADRAR network taken in our case study. The ADRAR distribution system is considered the third test system in this study. Additionally, it represents the ADRAR distribution network of the SDS (Southern Electricity Distribution Company). The test system named ADRAR network composed of one transformer, 14 buses, 13 lines, and 7 loads, as it is shown in Fig. 17.

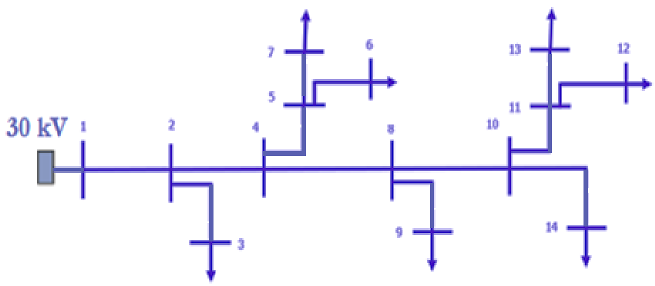

Fig. 17. ADRAR 14-Bus radial distribution system.

Total reactive and active loads at nominal load are 4.32 MVAr and 3.84 MW, respectively, at 30 kV and 80 MVA base values.

4.4.1. Case I : optimal integration of shunt capacitors

In the present scenario, the shunt capacitors just deliver reactive power into the network. Table 13, shows the impact of an optimal location of shunt capacitors using the cheetah optimization on the ADRAR power distribution system. The results of the power flow using BFS at nominal load show that the system devoid of shunt capacitors installation has an active network loss of 13.602 kW and a reactive network loss of 37.228 kVAr. Bus 13 has the lowest voltage magnitude of 0.9141 p.u. After optimal sizing and placement of shunt capacitors units with the Cheetah optimizer method, we can conclude that a single shunt capacitor placed on bus 10 of the network with a size of 258.16 kVAr saves 6.76 kW in active power losses and enhances the minimum voltage with a percentage of 5.97 % compared to the base case. In case II, the placement of two shunt capacitors on buses 11 and 2 in the ADRAR network, with sizes of 143.67 kVAr and 157.25 kVAr respectively, saves 7.05 kW in active power losses, with a percentage enhancement of the minimum voltage equal to 6.6%. In the third case, placement of three shunt capacitors on buses 12, 3, and 8 of the network with a size of 91.268, 87.281, and 121.969 kVAr respectively saves 7.131 kW in active power losses with a percentage enhancement of the minimum voltage equal to 6.63%.

Table 13. Comparison with different methods for integration of capacitor banks for ADRAR network.

Case	Method	SC size [kVAr]	Bus location	P_{loss} [kW]	P_{loss} [%]	Q_{loss} [kVAr]	V_{min} [p.u]	Bus location
Base case		/	/	13.602	/	37.228	0.9141	13
Case one 1 SC	CO (proposed)	258.16	10	6.842		18.205	0.9738	13
Case two 2 SCs	CO (proposed)	143.67 157.25	11 2	6.552		17.779	0.9801	14
Case three 3 SCs	CO (proposed)	91.268 87.281 121.969	12 3 8	6.471		17.665	0.9804	14

Fig. 18 demonstrates the voltage profiles of ADRAR distribution network with 14-bus. The voltage profile improves as the number of shunt capacitors increases. The insertion of shunt capacitors increases the minimum voltage from 0.9141 to 0.9804, resulting in improved voltage stability.

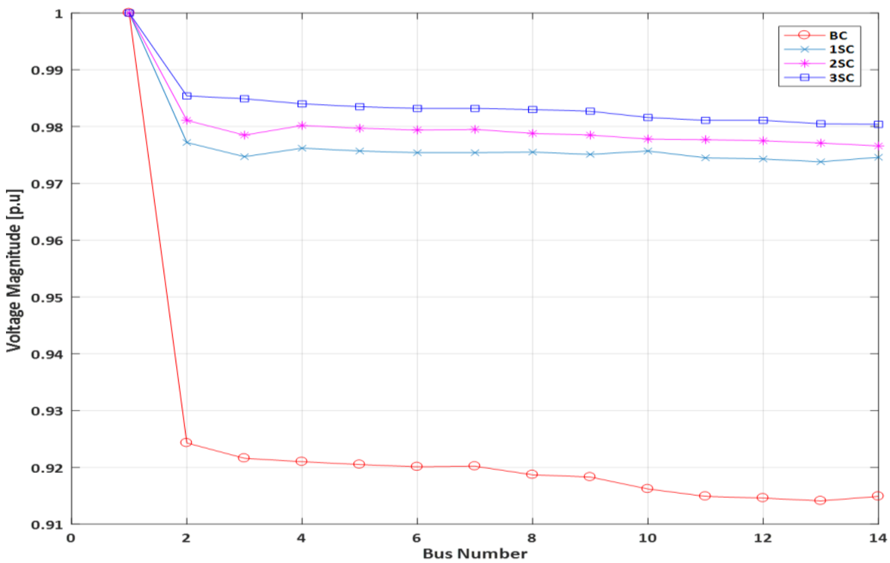

Fig. 18. Voltage distribution in ADRAR 14-bus system for different cases of shunt capacitors.

4.4.2. Case II : optimal integration of distributed generator with unity power factor

In the present scenario, the distributed generator only delivers active power into the network. Table 14 shows the impact of an optimal location of distributed generators using the cheetah optimization algorithm on the ADRAR power distribution system. In the first case, a single shunt capacitor placed on bus 8 of the network with a size of 252.178 kVAr saves 6.986 kW in active power losses and enhances the minimum voltage with a percentage of 2.29% compared to the base case.

Case II, placement of two distributed generators on buses 8 and 10 in the ADRAR network with a size of 153.132 kVAr and 129.3101 kVAr respectively saves 7.194 kW in active power losses with a percentage enhancement of the minimum voltage equal to 2.66 %. In third case, placement of three distributed generators on buses 8, 3, and 11 of the networks with a size of 116.191, 85.609 and 96.581 kVAr respectively saves 7.436 kW in active power losses with a percentage enhancement of the minimum voltage equal to 2.71%.

Table 14. Optimal results of Cheetah optimizer for ADRAR network at the unity power factor.

Case	Method	DG size [kW]	Location Bus	P_{loss} [kW]	P_{loss} [%]	Q_{loss} [kVAr]	V_{min} [p.u]	Location Bus
Base case		/	/	13.602	/	37.228	0.9141	13
Case one 1 DG	CO (proposed)	252.178	8	6.616		17.368	0.9370	13
Case two 2 DGs	CO (proposed)	153.132 129.310	8 10	6.408		16.858	0.9407	13
Case three 3 DGs	CO (proposed)	116.191 85.609 96.581	8 3 11	6.166		16.546	0.9412	13

Fig. 19 demonstrates the voltage profiles of ADRAR distribution network with 14-bus. The voltage profile improves as the number of distributed generators increases. The insertion of distributed generation increases the minimum voltage from 0.9141 p.u to 0.9412 p.u, resulting in improved voltage stability.

The application of the CO method to the ADRAR distribution network represents a significant validation in a real-world context; however, it is essential to consider the practical challenges encountered during its implementation. Among these challenges, computation time is a crucial factor, influenced by the network size and the complexity of the optimization process. Performance improvements could be achieved by refining the metaheuristic parameters or integrating computational acceleration techniques. Furthermore, adaptability to variable load profiles remains a major issue, as the optimization is performed based on specific conditions at a given moment. A potential improvement would involve integrating predictive models based on machine learning to anticipate demand fluctuations and dynamically adjust optimization strategies. Thus, while the obtained results demonstrate the effectiveness of the method, a deeper analysis of these limitations and potential solutions would enhance the robustness and relevance of the proposed approach.

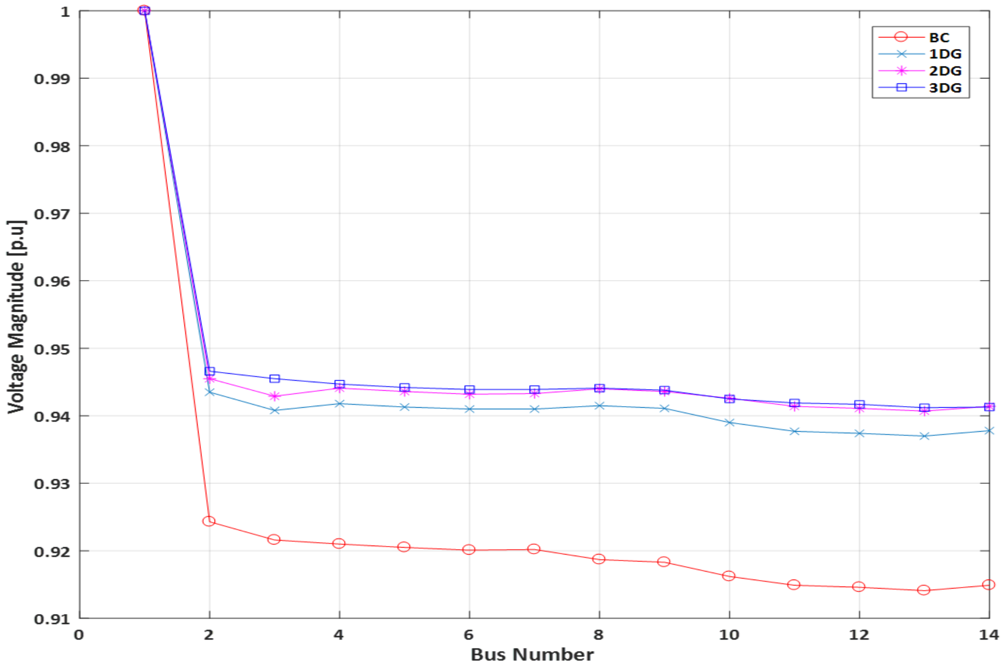

Fig. 19. Voltage distribution in ADRA 14-bus system for different cases of distributed generators.

The results obtained in this study highlight the superior performance of the Cheetah optimizer algorithm in reducing power losses and improving voltage profiles compared to other optimization methods such as the particle swarm optimization and the Salp Swarm Algorithm. This superiority can be attributed to the Cheetah optimizer algorithm's mechanism, which enables efficient search space navigation while preventing premature convergence. Specifically, the Cheetah optimizer method achieves greater loss reductions by adapting its step size and search intensity dynamically, allowing it to explore global optima in the early iterations and refine solutions in later stages. A key trade-off observed is between the number of iterations and solution accuracy. While a higher iteration count generally improves solution precision, excessive iterations may lead to diminishing returns in loss reduction. In our experiments, Cheetah optimizer demonstrated rapid convergence within 50 iterations, achieving power loss reductions of up to 37.34% for IEEE 33-bus and 35.50% for IEEE 69-bus with minimal computational overhead. Beyond this threshold, improvements were marginal, indicating an optimal balance between computational efficiency and solution quality. Additionally, the integration of adaptive mechanisms, such as the "sit and wait" strategy, enhances the algorithm's robustness against local optima, further justifying its effectiveness in real-world power distribution networks. These findings suggest that Cheetah optimizer is particularly well-suited for large-scale systems where computational efficiency and high solution accuracy are equally critical.

5. CONCLUSIONS

This study has introduced a Cheetah optimizer technique for the optimal sizing and allocation of shunt capacitors and distributed generation units, focusing on the reduction of both active and reactive power losses as well as the enhancement of voltage profiles. The efficacy of Cheetah optimizer was evaluated and confirmed; additionally, results of this study indicated that the proposed methodology yields enhanced performance with optimal outcomes within all scenarios and constraints. The proposed method was implemented on various test systems, including the "IEEE 33-Bus" radial distribution system, the "IEEE 69-Bus" radial distribution system, and the ADRAR distribution network in Southern Algeria. The proposed Cheetah optimizer is a meta-heuristic optimization method inspired by the foraging behavior of cheetahs in their natural habitat. This study encompasses the following simulations: Case I involves the integration of one, two, or three shunt capacitors; Case II examines a variable load with three distinct load levels using three distributed generators for the IEEE 33-bus network and two shunt capacitors for the IEEE 69-bus network and Case III entails the insertion of one, two, or three distributed generators. The outcomes obtained from the proposed Cheetah optimizer are compared with the results of bat algorithm, moth flame optimization algorithm, hybrid sine cosine algorithm, cuckoo search algorithm, constriction-factor particle Swarm Optimization, parameter improved particle swarm optimization, hybrid sequential quadratic programming, improved northern goshawk optimization, northern goshawk optimization, enhanced grasshopper optimization algorithm, improved golden jackal optimization algorithm, tasmanian devil optimization, and coyote optimization algorithm. The obtained numerical results indicate that proposed Cheetah optimizer performance surpasses the aforesaid approaches.

REFERENCES

[1] M. El-Hawary, “The smart grid—state-of-the-art and future trends,” *Electric Power Components and Systems*, vol. 42, no. 3–4, pp. 239–250, 2014, doi: 10.1080/15325008.2013.868558.

[2] N. Kanwar, N. Gupta, K. Niazi, A. Swarnkar,”Optimal allocation of distributed energy resources using improved meta-heuristic techniques, ” *Electric Power Components and Systems*, vol. 44, no. 13, pp. 1466–1477, 2016, doi: 10.1080/15325008.2016.1172682.

[3] A. ALAhmad, “Voltage regulation and power loss mitigation by optimal allocation of energy storage systems in distribution systems considering wind power uncertainty,” *Journal of Energy Storage*, vol. 59, no. December 2022, pp. 106467, 2023, doi: 10.1016/j.est.2022.106467.

[4] D. Hung, N. Mithulananthan, ”Loss reduction and loadability enhancement with DG: a dual-index analytical approach,” *Applied Energy*, vol. 115, pp. 233–241, 2014, doi: 10.1016/j.apenergy.2013.11.010.

[5] M. Cikan, B. Kekezoglu, ”Comparison of metaheuristic optimization techniques including Equilibrium optimizer algorithm in power distribution network reconfiguration, ” *Alexandria Engineering Journal*, vol. 61, no 2, pp. 991-1031, 2022, doi: 10.1016/j.aej.2021.06.079.

[6] M. Shaik, P. Mareddy, N. Visali, ”Enhancement of voltage profile in the distribution system by reconfiguring with DG placement using equilibrium optimizer,” *Alexandria Engineering Journal*, vol. 61, pp. 4081–4093, 2022, doi: 10.1016/j.aej.2021.09.063.

[7] N T. guyen, T. Nguyen, N. Nguyen, T. Duong, ”A novel method based on coyote algorithm for simultaneous network reconfiguration and distribution generation placement, ”*Ain Shams Engineering Journal*, vol. 12, no. 1, pp. 665–676, 2020, doi: 10.1016/j.asej.2020.06.005.

[8] S. Kansal, V. Kumar, B. Tyagi,” Optimal placement of different type of DG sources in distribution networks, ” *International Journal of Electrical Power & Energy Systems*, vol. 53, pp. 752–760, 2013, doi: 10.1016/j.ijepes.2013.05.040.

[9] P. Moghari, R. Chabanloo, H. Torkaman, ”Distribution system reconfiguration based on MILP considering voltage stability,” *Electric Power Systems Research*, vol. 222, p. 109523, 2023, doi: 10.1016/j.epsr.2023.109523.

[10] I. Hamida, S. Salah, F. Msahli, M. Mimouni. ′′Optimal network reconfiguration and renewable DG integration considering time sequence variation in load and DGs," *Renewable Energy*, vol. 121, pp. 66–80, 2018, doi: 10.1016/j.renene.2017.12.106.
[11] U. Raut, S. Mishra, "An improved sine–cosine algorithm for simultaneous network reconfiguration and DG allocation in power distribution systems," *Applied Soft Computing*, vol. 92, p. 106293, 2020, doi: 10.1016/j.asoc.2020.106293.
[12] S. Essallah, A. Khedher, "Optimization of distribution system operation by network reconfiguration and DG integration using MPSO algorithm," *Renewable Energy Focus*, vol. 34, pp. 37–46, 2020, doi: 10.1016/j.ref.2020.04.002.
[13] N. Kanwar, N. Gupta, K. Niazi, A. Swarnkar, "Improved cat swarm optimization for simultaneous allocation of DSTATCOM and DGS in distribution systems," *Journal of Renewable Energy*, pp. 1–10, 2015, doi: 10.1155/2015/189080.
[14] M. Khasanov, S. Kamel, H. Hasanien, A. Al-Durra, "Rider optimization algorithm for optimal DG allocation in radial distribution network" International Conference on Smart Power & Internet Energy Systems, 2020, doi: 10.1109/SPIES48661.2020.9243103.
[15] R. Sellami, F. Sher, R. Neji, "An improved MOPSO algorithm for optimal sizing & placement of distributed generation: a case study of the Tunisian offshore distribution network (ASHTART)," *Energy Reports,* vol. 8, pp. 6960–6975, 2022, doi: 10.1016/j.egyr.2022.05.049.
[16] T. Yuvaraj, T. Suresh, U. Meyyappan, B. Aljafari, S. Thanikanti, "Optimizing the allocation of renewable DGs, DSTATCOM, and BESS to mitigate the impact of electric vehicle charging stations on radial distribution systems," *Heliyon*, vol. 9. no. 12, p. e23017, 2023, doi: 10.1016/j.heliyon.2023.e23017.
[17] K. Sambaiah, T. Jayabarathi, "Optimal reconfiguration and renewable distributed generation allocation in electric distribution systems," *International Journal of Ambient Energy*, vol. 42, no. 9, pp. 1018–1031, 2019, doi: 10.1080/01430750.2019.1583604.
[18] A. Youssef, S. Kamel, M. Ebeed, J. Yu, "Optimal capacitor allocation in radial distribution networks using a combined optimization approach," *Electric Power Components and Systems*, vol. 46, no. 19–20, pp. 2084–2102, 2018, doi: 10.1080/15325008.2018.1531956.
[19] R. Arunjothi, K. Meena, "Optimizing capacitor size and placement in radial distribution networks for maximum efficiency," *Systems and Soft Computing*, vol. 6, p. 200111, 2024, doi: 10.1016/j.sasc.2024.200111.
[20] S. Salimon, O. Omofuma, O. Akinrogunde, T. Thomas, T. Edwin, "Optimal allocation of shunt capacitors in radial distribution networks using constriction-factor particle swarm optimization and its techno-economic analysis," *Franklin Open*, vol. 7, p. 100093, 2024, doi:1016/j.fraope.2024.100093.
[21] S. Injeti, V. Thunuguntla, M. Shareef, "Optimal allocation of capacitor banks in radial distribution systems for minimization of real power loss and maximization of network savings using bio-inspired optimization algorithms," *International Journal of Electrical Power & Energy Systems*, vol. 69, pp. 441–455, 2015, doi: 10.1016/j.ijepes.2015.01.040.
[22] M. El-Saeed, A. Abdel-Gwaad, M. Farahat, "Solving the capacitor placement problem in radial distribution networks," *Results in Engineering*, vol. 17, p. 100870, 2022, doi: 10.1016/j.rineng.2022.100870.
[23] M. Mahdavi, A. Awaafo, M. Dini, S. Moradi, F. Jurado, D. Vera, "A flexible loss reduction formulation for simultaneous capacitor placement and network reconfiguration in distribution grids," *Electric Power Systems Research*, vol. 235, p. 110708, 2024, doi: 10.1016/j.epsr.2024.110708.
[24] A. El-Ela, R. El-Sehiemy, A. Kinawy, M. Mouwafi, "Optimal capacitor placement in distribution systems for power loss reduction and voltage profile improvement," *IET Generation Transmission & Distribution*, vol. 10, no. 5, pp. 1209–1221, 2016, doi: 10.1049/iet-gtd.2015.0799.

[25] S. Angalaeswari, P. Sanjeevikumar, K. Jamuna, Z. Leonowicz, "Hybrid PIPSO-SQP algorithm for real power loss minimization in radial distribution systems with optimal placement of distributed generation," *Sustainability*, vol. 12, no. 14, p. 5787, 2020, doi: 10.3390/su12145787.

[26] G. Chen, J. Li, Y. Xu, B. Peng, H. Tan, H. Long, "Optimal configuration of renewable energy DGs based on improved northern goshawk optimization algorithm considering load and generation uncertainties," *Engineering Letters*, vol. 31, no. 2, 2023, https://api.semanticscholar.org/CorpusID:271596411

[27] H. Manafi, N. Ghadimi, M. Ojaroudi, P. Farhadi, "Optimal placement of distributed generations in radial distribution systems using various PSO and DE algorithms," *Electronics and Electrical Engineering*, vol. 19, no. 10, pp. 53-57, 2013, doi: 10.5755/j01.eee.19.10.1941.

[28] S. Sudabattula, "Optimal allocation of solar based distributed generators in distribution system using Bat algorithm," *Perspectives in Science*, vol. 8, pp. 270-272, 2016, doi: 10.1016/j.pisc.2016.04.048.

[29] S. Velamuri, S. Cherukuri, S. Sudabattula, N. Prabaharan, E. Hossain, "Combined approach for power loss minimization in distribution networks in the presence of gridable electric vehicles and dispersed generation," *IEEE Systems Journal*, vol. 16, no. 2, pp. 3284-3295, 2022, doi: 10.1109/JSYST.2021.3123436.

[30] M. Elseify, F. Hashim, A. Hussien, H. Abdel Mawgoud, S. Kamel, "Single and multi-objectives based on an improved golden jackal optimization algorithm for simultaneous integration of multiple capacitors and multi-type DGs in distribution systems," *Applied Energy*, vol. 353, p. 122054, 2023, doi: 10.1016/j.apenergy.2023.122054.

[31] M. Elseify, F. Hashim, A. Hussien, S. Kamel, "Boosting prairie dog optimizer for optimal planning of multiple wind turbine and photovoltaic distributed generators in distribution networks considering diferent dynamic load models," *Scientific Reports*, vol. 14, p. 14173, 2024, doi: 10.1038/s41598-024-64667-4.

[32] A. Bayat, A. Bagheri, "Optimal active and reactive power allocation in distribution networks using a novel heuristic approach," *Applied Energy*, vol. 233–234, pp. 71–85, 2019, doi.org/10.1016/j.apenergy.2018.10.030.

[33] A. Rohollah, A. Morteza, "Optimal allocation of distributed generation and distribution static compensator using improved multi-objective function and info optimization algorithm," *Jordan Journal of Electrical Engineering*, vol. 11, no. 1, pp. 112-130, 2025, doi: 10.5455/jjee.204-1720231510.

[34] Tandon, S. Nawaz, ''Optimal integration of PV-based distributed generators and shunt capacitors for 69 bus system using imperialist competitive algorithm and ETAP software,'' *Jordan Journal of Electrical Engineering*, vol. 9, no. 3, pp. 301-321, 2023, doi: 10.5455/jjee.204-1670927775.

[35] J. Ruba, S. Ganesh, "Power flow analysis for radial distribution systems using backward/forward sweep method," *International Journal of Electrical and Computer Engineering*, vol. 8, no. 10, pp. 1621–1625, 2014, doi: 10.5281/zenodo.1337731.

[36] S. Brien, W. Johnson, C. Driscoll, P. Dobrynin, L. Marker. "Conservation genetics of the cheetah: lessons learned and new opportunities," *Journal of Heredity*, vol. 108, pp. 671–67, 2017, doi: /10.1093/jhered/esx047.

[37] L. Marker, L. Boast, A. Schmidt-Küntzel, *Cheetahs: Biology and Conservation*, Academic Press, 2018.

[38] P. Krausman, S. Morales, ''Acinonyx jubatus,'' *Mammalian Species*, vol. 771, no. 1, pp.1-6, 2005, doi: 10.1644/1545-1410

[39] R. Estes, *The Behavior Guide to African Mammals: Including Hoofed Mammals, Carnivores*, Primates, University of California Press, 2012.

[40] A. Patel, M. Braae, "Rapid turning at high-speed: Inspirations from the cheetah's tail,'' International Conference on Intelligent Robots and Systems, 2013, doi: 10.1109/IROS.2013.6697154.

[41] R. Aarde, A. Dyk, "Inheritance of the king coat colour pattern in cheetahs Acinonyx jubatus," *Journal of Zoology*, vol. 209, no. 4, pp. 573–578, 1986, doi: 10.1111/j.1469-7998.1986.tb03612.x.

[42] J. Phillips, "Bone consumption by cheetahs at undisturbed kills: evidence for a lack of focal-palatine erosion,'' *Journal of Mammalogy*, vol. 74, pp. 487–492, 1993, doi: 10.2307/1382408.

[43] G. Dhiman, V. Kumar, "Emperor penguin optimizer: a bio-inspired algorithm for engineering problems," *Knowledge-Based Systems*, vol. 159, pp. 20–50, 2018, doi: 10.1016/j.knosys.2018.06.001.

[44] M. Akbari, M. Zare, R. Abarghooee, S. Mirjalili, M. Deriche, "The cheetah optimizer: a nature-inspired metaheuristic algorithm for large-scale optimization problems," *Scientific Reports*, vol. 12, no. 1, 2022, doi: 10.1038/s41598-022-14338-z.

[45] M. Aman, G. Jasmon, A. Bakar, H. Mokhlis, "Optimum network reconfiguration based on maximization of system loadability using continuation power flow theorem," *International Journal of Electrical Power & Energy Systems*, vol. 54, pp. 123-133, 2013, doi: 10.1016/j.ijepes.2013.06.026.

[46] S. Gopiya Naik, D. Khatod, M. Sharma, "Optimal allocation of combined DG and capacitor for real power loss minimization in distribution networks," *International Journal of Electrical Power Energy Syst*em, vol. 53, pp. 967–973, 2013, doi: 10.1016/j. ijepes.2013.06.008.

[47] T. Yuvaraj, K. Devabalaji, S. Srinivasan, N. Prabaharan, R. Hariharan, H. Alhelou, B. Ashokkumar, "Comparative analysis of various compensating devices in energy trading radial distribution system for voltage regulation and loss mitigation using blockchain technology and bat algorithm," *Energy Reports*, vol. 7, pp. 8312–8321, 2021, doi: 10.1016/j.egyr.2021.08.184.

[48] H. Abdel-Mawgoud, S. Kamel, A. El-Ela, F. Jurado, "Optimal allocation of DG and capacitor in distribution networks using a novel hybrid MFO-SCA method,'' *Electrical Power Components and Systems*, vol. 49, no. 3, pp. 259–275, 2021, doi: 10.1080/ 15325008.2021.1943066.

[49] K. Devabalaji, T. Yuvaraj, K. Ravi, "An efficient method for solving the optimal sitting and sizing problem of capacitor banks based on cuckoo search algorithm," *Ain Shams Engineering Journal*, vol. 9, no. 4, pp. 589–597, 2018, doi: 10.1016/j. asej.2016.04.005.

[50] R. Arulraj, N. Kumarappan, "Optimal economic-driven planning of multiple DG and capacitor in distribution network considering different compensation coefficients in feeder's failure rate evaluation," *Engineering Science and Technology an International Journal*, vol. 22. no. 1, pp. 67–77, 2018, doi: 10.1016/j.jestch.2018.08.009.

[51] S. Biswal, G. Shankar, "Optimal sizing and allocation of capacitors in radial distribution system using sine cosine algorithm" IEEE International Conference on Power Electronics, Drives and Energy Systems, 2018, doi: 10.1109/PEDES.2018.8707739.

[52] S. Kansal, V. Kumar, B. Tyagi, "Hybrid approach for optimal placement of multiple DGs of multiple types in distribution networks," *International Journal of Electrical Power & Energy Systems*, vol. 75, pp. 226–235, 2016, doi: 10.1016/j.ijepes.2015.09.002.

[53] L. Kien, T. Nguyen, B. Dinh, T. Nguyen, "Optimal reactive power generation for radial distribution systems using a highly effective proposed algorithm," *Complexity*, vol. 1, 2021, doi: 10.1155/2021/2486531.

[54] I. Abril, "Algorithm of inclusion and interchange of variables for capacitors placement," *Electric Power Systems Research*, vol. 148, pp. 117–126, 2017, doi: 10.1016/j.epsr.2017.03.027.

[55] V. Tamilselvan, T. Jayabarathi, T. Raghunathan, X. Yang, "Optimal capacitor placement in radial distribution systems using flower pollination algorithm," *Alexandria Engineering Journal*, vol. 57, no. 4, pp. 2775–2786, 2018, doi: 10.1016/j.aej.2018.01.004.

[56] D. Hung, N. Mithulananthan, R. Bansal, "A combined practical approach for distribution system loss reduction," *International Journal of Ambient Energy*, vol. 36, no. 3, pp. 123–131, 2015, doi: 10.1080/01430750.2013.829784.

[57] S. Kamel, A. Amin, A. Selim, M. Ahmed, "Optimal placement of DG and capacitor in radial distribution systems considering load variation" International Conference on Computer, Control, Electrical, and Electronics Engineering, 2019, doi: 10.1109/iccceee46830.2019.9071384.